CHEMICAL SPECIATION OF ZINC AND LEAD IN SOILS AND ITS EFFECTS ON BIOACCESSIBILITY

A Thesis Submitted to the College of Graduate Studies and Research

in Partial Fulfillment of the Requirements

For the Degree of Master of Science

in the Department of Soil Science

University of Saskatchewan

Saskatoon

By

Essouassi Elikem

PERMISSION TO USE

In presenting this thesis in partial fulfilment of the requirements for a Postgraduate degree from the University of Saskatchewan, I agree that the Libraries of this University may make it freely available for inspection. I further agree that permission for copying of this thesis in any manner, in whole or in part, for scholarly purposes may be granted by the professor or professors who supervised my thesis work or, in their absence, by the Head of the Department or the Dean of the College in which my thesis work was done. It is understood that any copying or publication or use of this thesis or parts thereof for financial gain shall not be allowed without my written permission. It is also understood that due recognition shall be given to me and to the University of Saskatchewan in any scholarly use which may be made of any material in my thesis.

Requests for permission to copy or to make other use of material in this thesis in whole or part should be addressed to:

Head, Department of Soil Science
University of Saskatchewan
51 Campus Drive
Saskatoon, Saskatchewan S7N 5A8

ABSTRACT

Soils with metal concentrations above regulatory guidelines (e.g., Canadian Soil Quality Guidelines) may pose health risks to humans (especially children), plants, animals and soil microorganisms. To study the toxicity and assess the risks of metal contaminated soils to the aforementioned receptors, researchers add metal salts to uncontaminated soils. This commonly used method of metal addition to soils sometimes fails to mimic field contaminated soils with regards to metal concentration and speciation. In addition, it creates artifacts that may skew metal toxicity and risk assessment results. Consequently, two alternative solid metal addition methods (annealed metal and metal oxide) were compared to the widely used metal-salt method. The objective was to identify the method that adequately mimics environmentally relevant Zn, Pb and Ni concentrations and Zn speciation.

After spiking three soils with three different metal mixtures and incubating for 30 days, total metal concentration in the spiked soils were measured with X-ray fluorescence (XRF); Zn speciation was characterized using X-ray powder diffraction (XRD) and X-ray absorption near edge structure (XANES) spectroscopy. Speciation of Zn depended on spiking method and soil properties, especially pH. Each spiking method produced between 1-3 Zn species that occur in smelter-affected soils. Comparatively, the metal-salt spiking method failed to replicate the environmentally relevant Zn and Ni concentrations. Also, it was found to have several drawbacks that may present serious challenges to toxicity and risk assessment research. The oxide spiking method produced metal concentrations that were higher than the expected values. The acidic pH of the test soils ensured the dissolution of ZnO, which led to the formation of secondary Zn species. Franklinite was the synthetic mineral produced from the annealing process and it was found to be very stable even at pH 3.4. None of the metal addition methods evaluated in this study adequately mimicked the selected field conditions.

The hypothesis that metal bioaccessibility is controlled by metal speciation and not metal concentration was tested in the second part of this study. A combination of bioaccessibility extractions, XANES and LCF were used to identify the species of Zn

and Pb in the spiked and smelter-affected soils that contribute Zn and Pb ions towards bioaccessibility. After conducting *in vitro* digestion tests on the soil samples, XANES and LCF analyses were carried out on the residual pellets to identify the species of Zn and Pb that remained after digestion of the soils in pH 1.4 and 6.3 gastric and duodenal fluids, respectively. In the residual pellets from the simulated stomach, ZnO, sphalerite (ZnS), outer-sphere Zn, PbO, and hydrocerussite [$Pb_3(CO_3)_2(OH)_2$] were below detection limits, indicating that the total metal fraction of these species contributed to the bioaccessible metal concentrations in the stomach. The high relative abundance of some of these metal species (e.g., ZnO) translated to high bioaccessible metal concentrations. Conversely, franklinite ($ZnFe_2O_4$) and Zn incorporated into a hydroxy interlayered mineral (Zn-HIM) were detected in the residual pellets from both the simulated stomach and duodenum. This suggests that franklinite and Zn-HIM are sparingly soluble, and released relatively low concentrations of Zn ions into the digestive fluids. The residence time of Zn-Al layered double hydroxide (Zn-Al LDH) in soils was found to affect the release of Zn ions into the simulated digestive fluids. One field sample (stabilized soil) and one spiked sample (oxide spiked WTRS soil) contained Zn-Al LDH; however, after digestion, Zn-Al LDH was detected in residual pellets of the field sample, but not the spiked sample. The resistance of Zn-Al LDH in the field sample to dissolution is probably due to longer residence time, which allowed silication in the hydroxide layers.

TABLE OF CONTENTS

PERMISSION TO USE i

ABSTRACT ii

LIST OF TABLES vi

LIST OF FIGURES vii

LIST OF ABBREVIATIONS x

1 INTRODUCTION 1

2 LITERATURE REVIEW 4
- 2.1 **Human Health Risk Assessment (HHRA)** . . . 4
- 2.2 **Speciation of metals in soils** . . . 6
  - 2.2.1 Sorption/desorption of metals in soils . . . 6
  - 2.2.2 Precipitation/dissolution of metals in soils . . . 9
  - 2.2.3 Reduction/oxidation of metals in soil . . . 10
- 2.3 **X-ray Absorption Spectroscopy (XAS)** . . . 11
- 2.4 **X-ray diffraction (XRD)** . . . 14

3 EVALUATION OF SOIL SPIKING METHODS 16
- 3.1 **Preface** . . . 16
- 3.2 **Abstract** . . . 17
- 3.3 **Introduction** . . . 18
- 3.4 **Materials and Methods** . . . 19
  - 3.4.1 Soil samples . . . 19
  - 3.4.2 Spiking with metal nitrates and leaching . . . 20
  - 3.4.3 Spiking with synthetic minerals . . . 21
  - 3.4.4 Spiking with metal oxides . . . 21
  - 3.4.5 X-ray diffraction (XRD) analysis . . . 22
  - 3.4.6 X-ray fluorescence (XRF) analysis . . . 22
  - 3.4.7 X-ray absorption spectroscopy (XAS) analysis . . . 22
- 3.5 **Results and Discussion** . . . 23
  - 3.5.1 Phase identification of synthetic minerals . . . 23
  - 3.5.2 Total Zn, Pb and Ni concentrations in spiked soils . . . 25
  - 3.5.3 Zn speciation in spiked soils . . . 29
  - 3.5.4 Implications for risk assessment and soil toxicity studies . . . 33
- 3.6 **Conclusion** . . . 34

4 EFFECTS OF CHEMICAL SPECIATION ON THE BIOACCESSIBILITY OF ZINC AND LEAD IN SPIKED AND SMELTER-AFFECTED SOILS 36

4.1 **Preface** . . . 36
4.2 **Abstract** . . . 37
4.3 **Introduction** . . . 38
4.4 **Materials and Methods** . . . 39
4.4.1 Soil samples and treatments . . . 39
4.4.2 *In vitro* gastric model . . . 40
4.4.3 *In vitro* duodenal model . . . 41
4.4.4 Chemical analysis . . . 41
4.4.5 Statistical Analysis . . . 41
4.4.6 X-ray absorption spectroscopy (XAS) analysis . . . 42
4.5 **Results** . . . 43
4.5.1 Zn and Pb bioaccessibility . . . 43
4.5.2 Zn speciation in residual pellets . . . 47
4.6 **Discussion** . . . 54
4.6.1 Metal species that contribute to bioaccessible concentrations . . . 54
4.6.2 Implications for risk assessment and soil remediation . . . 58
4.7 Conclusions . . . 59

5 SYNTHESIS AND CONCLUSIONS **61**

6 REFERENCES **65**

A Appendix **72**

List of Tables

Table 3.1 Mineralogy and chemical properties of reference soils. 20

Table 3.2 Source and concentration of metal mixtures. 21

Table 3.3 Total Zn concentrations and Linear Combination fits of the XANES from 3.22, WTRS and UBC spiked soils. 31

Table 4.1 Total Zn and Pb concentrations in the 27 spiked soils used for the bioaccessibility measurements. 40

Table 4.2 Total and bioaccessible Zn concentrations and XANES Linear Combination fits (LCF) results for the smelter-affected soils (stabilized and eroding) and residual pellets. 50

Table 4.3 Total and bioaccessible Zn concentrations and XANES Linear Combination fits (LCF) results for 3.22 spiked soil and residual pellets. 51

Table 4.4 Total and bioaccessible Zn concentrations and XANES Linear Combination fits (LCF) results for WTRS spiked soil and residual pellets. 52

Table 4.5 Total and bioaccessible Zn concentrations and XANES Linear Combination fits (LCF) results for UBC spiked soil and residual pellets. 53

Table A.1 ANOVA table: gastric Zn bioaccessibility 73

Table A.2 ANOVA table: duodenal Zn bioaccessibility 74

Table A.3 ANOVA table: gastric Pb bioaccessibility 75

Table A.4 ANOVA table: gastric Pb bioaccessibility 76

LIST OF FIGURES

Fig. 2.1 Speciation of metals in soils. Adapted from Adamo et al. (2008) 7

Fig. 2.2 Zn k-edge XAS spectrum, showing the X-ray absorption near edge structure (XANES) and extended X-ray absorption fine structure (EXAFS). 12

Fig. 2.3 Example of LCF modeling of Zn k-edge XANES spectrum of soil sample (black + symbols). The best fit LCF is shown in red, and the three standard compounds: franklinite, aqueous Zn, and Zn-adsorbed on goethite and their relative contributions to the experimental spectrum are shown below the fit. 14

Fig. 3.1 X-ray powder diffraction pattern of synthetic minerals; (a), (b), and (c) represent synthetic minerals produced from Flin Flon, Port Colborne, and Sudbury mixtures, respectively. 24

Fig. 3.2 Background corrected total Zn concentration in 3.22, WTRS, and UBC spiked soils; (a), (b), and (c) represent Flin Flon, Port Colborne and Sudbury mixtures, respectively. The target concentrations, which the spiking methods were expected to replicate, were derived from Flin Flon, Port Colborne, and Sudbury smelter-affected soils. 26

Fig. 3.3 Background corrected total Ni concentration in 3.22, WTRS, and UBC spiked soils; (a), (b), and (c) represent Flin Flon, Port Colborne and Sudbury mixtures, respectively. The target concentrations, which the spiking methods were expected to replicate, were derived from Flin Flon, Port Colborne, and Sudbury smelter-affected soils. 27

Fig. 3.4 Background corrected total Ni concentration in 3.22, WTRS, and UBC spiked soils; (a), (b), and (c) represent Flin Flon, Port Colborne and Sudbury mixtures, respectively. The target concentrations, which the spiking methods were expected to replicate, were derived from Flin Flon, Port Colborne, and Sudbury smelter-affected soils. 28

Fig. 3.5 Bulk Zn K-edge XANES spectra (black lines) and linear combination fits (LCF) (red lines) for 3.22, WTRS, and UBC spiked (annealed, oxide and nitrate) soil samples. Zn K-edge XANES spectra were collected from soils spiked with Flin Flon mixture. LCF results are provided in Table 3.3. 30

Fig. 4.1 Bioaccessible Zn concentrations compared across 3 factors: mixture (Flin Flon, Sudbury and Port Colborne), spiking method (oxide, annealed, and nitrate) and soil (3.22, UBC, and WTRS). Since time was not a significant predictor of bioaceessibility, only bioaccessible concentrations after 120 and 240 minutes are presented in this graph for stomach and duodenum, respectively. (a) represents stomach and (b) duodenum. Bars with the same lowercase alphabets are not significantly different. 45

Fig. 4.2 Bioaccessible Pb concentrations compared across 3 factors: mixture (Flin Flon, Sudbury and Port Colborne), spiking method (oxide, annealed, and nitrate) and soil (3.22, UBC, and WTRS). Since time was not a significant predictor of bioaceessibility, only bioaccessible concentrations after 120 and 240 minutes are presented in this graph for stomach and duodenum, respectively. (a) represents stomach and (b) duodenum. Bars with the same lowercase alphabets are not significantly different. 46

Fig. 4.3 Zn K-edge XANES spectra (black lines) and linear combination fits (red lines) for (a) smelter-affected soils (stabilized and eroding) from Flin Flon, MB, and their respective gastric and duodenal residual pellets; (b), (c) and (d) represent 3.22, WTRS and UBC spiked (annealed, nitrate and oxide) soils, respectively and their corresponding gastric and duodenal residual pellets. LCF results are provided in Tables 4.2, 4.3, 4.4 and 4.5 for (a), (b), (c), and (d), respectively. 49

Fig. A.1 Zn reference standards bulk XANES used in linear combination fitting of spiked and smelter-affected soils, and residual pellets. . 72

Fig. A.2 Percent Zn compared across 3 factors: mixture (Flin Flon, Sudbury and Port Colborne), spiking method (oxide, annealed, and nitrate) and soil (3.22, UBC, and WTRS). Since time was not a significant predictor of bioaceessibility, only bioaccessible concentrations after 120 and 240 minutes are presented in this graph for stomach and duodenum, respectively. (a) represents stomach and (b) duodenum. Bars with the same lowercase alphabets are not significantly different. Calculation of % Zn bioaccessibility was based on the assumption that 0.1 g of soil was removed at each sampling point. 77

Fig. A.3 Percent Pb bioaccessibility compared across 3 factors: mixture (Flin Flon, Sudbury and Port Colborne), spiking method (oxide, annealed, and nitrate) and soil (3.22, UBC, and WTRS). Since time was not a significant predictor of bioaceessibility, only bioaccessible concentrations after 120 and 240 minutes are presented in this graph for stomach and duodenum, respectively. (a) represents stomach and (b) duodenum. Bars with the same lowercase alphabets are not significantly different. Calculation of % Zn bioaccessibility was based on the assumption that 0.1 g of soil was removed at each sampling point. 78

List of Abbreviations

CEC	Cation Exchange Capacity
CLS	Canadian light source Synchrotron
CMCF	Canadian Macromolecular Crystallography Facility
EXAFS	Extended X-ray absorption fine structure
GIT	Gastrointestinal tract
HHRA	Human Health Risk Assessment
HXMA	Hard X-ray MicroAnalysis
LCF	Linear combination fitting
LME	Linear mixed-effects
PBET	Physiologically based extraction test
PQRA	Primary Qualitative Risk Assessment
PZC	Point of Zero Charge
SHIME	Simulator of the human intestinal microbial ecosystem
SSRA	Site specific Risk Assessment
USEPA	United States Environmental Protection Agency
XAS	X-ray absorption spectroscopy
XAFS	X-ray absorption fine structure
XANES	X-ray absorption near edge structure
XRF	X-ray fluorescence
Zn-Al LDH	Zinc aluminum layered double hydroxide
Zn-Al-HIM	Zinc aluminum hydroxy interlayer mineral

1 INTRODUCTION

Metals are central to everyday life and economic development because of characteristics such as high strength, durability, capacity to conduct electricity and heat. These properties make metals suitable for industrial, agricultural, medical, pharmaceutical and technological applications. However, the widespread use of metals has resulted in their wide distribution in the environment, raising concerns over their potential adverse impacts on human and environmental health. The pervasiveness of metal contamination is due primarily to their multiple paths for introduction into the environment: mining and smelting activities, industrial emissions, atmospheric deposition, sewage irrigation, inadequate waste management, domestic effluents and the use of certain pesticides and phosphate fertilizers. According to the International Council on Mining and Metals (ICMM), the concentrations of metals in the environment are expected to rise as increase in global population and material standard of living increase the demand for metals (ICMM, 2012).

Some metals (e.g., Fe, Cr, Co, Zn, Se, Cu, Mo, and Mn) are required by humans and other living organisms in trace amounts to maintain physiological and biochemical processes. Inadequate supply of these essential trace elements could lead to deficiency syndromes (WHO, 1996). However, when the concentration of these metals exceeds what is required, adverse effects are likely to occur. Other metals including Lead (Pb), arsenic (As), mercury (Hg), nickel (Ni), and cadmium (Cd) have no known biological significance. Instead, they are deleterious to humans, and many essential organisms in the ecosystem even at low levels of exposure. For instance, both organic and inorganic Pb compounds are neurotoxic, affecting the central nervous system by inducing memory loss, short attention span, and dizziness. In extreme cases, Pb encephalopathy can result in hallucinations, delirium, convolutions, coma, and death, especially in children. Additionally, long-term exposure to low levels of Pb can impair cognitive development in children (Apostoli et al., 2006) . Zinc and Copper are gastrointestinal irritants; they erode the lining of the gastrointestinal tract (GIT) (Nriagu, 2011). Inhalation of zinc oxide fumes have strongly been linked to the development of metal

fume fever, a condition commonly found in welders (Barceloux & Barceloux, 1999b). Epidemiological studies have shown that Ni roasting, calcining, and sintering operations exposes workers to nickel oxides and sulfides; inhalation of these compounds increases the risk of upper respiratory track cancer (Barceloux & Barceloux, 1999a).

In general, the toxicity of a metal contaminant depends on the amount of metal that is absorbed into systemic circulation. This amount, known as the bioavailable fraction, is an important parameter in exposure equations during human and ecological risk assessment of metal contaminated sites (Health Canada, 2010). The bioavailable fraction is obtained through *in vivo* animal feeding studies, which are laborious, expensive and plagued with ethical issues. For these reasons, *in vitro* gastrointestinal models have been developed to provide conservative estimates of bioavailability. Incidental ingestion of soil is a major route through which humans, especially children, become exposed to metals. In this case, the gastrointestinal models determine the bioaccessible fractions, which is the amount of metal released into the GIT and is available for absorption via the intestinal epithelium (USEPA, 2007).

Currently, risk assessment of metal contaminated sites is predicated on the assumption that, the total metal content in a given mass of soil is bioaccessible (Scheckel et al., 2009; Koch et al., 2013). For instance, regulatory guidelines for arsenic assumes 100% bioaccessibility; however, many studies have demonstrated that this is not possible because of matrix effects and natural attenuation processes (Scheckel, Chaney, Basta, & Ryan, 2009). Although the total metal content is indicative of the degree of contamination and an important parameter in assessing the risks posed by contaminated sites, it has weak predictive power with regards to bioaccessibility and bioavailability (Sparks, 2003; Scheckel et al., 2009). This is because the desorption of metals from soil particles into an aqueous medium surrounding it (e.g., soil water and gastric fluid) is controlled by soil properties including soil texture, pH, cation exchange capacity, redox conditions, organic matter content, the presence of anionic species (such as carbonates, phosphates, chloride, sulfides hydroxides and organic acids) that form complexes with metal cations, and the duration of contact between the metal and soil particles (Richardson et al., 2006). Thus, understanding the interactions between these soil properties and metal contaminants will allow for the identification of metal

species that are present in contaminated soils and hence the metal species that will likely contribute to bioaccessibility. Synchrotron techniques such as X-ray absorption near edge structure (XANES) and X-ray absorption fine structure (XAFS) together with statistical methods such as linear combination fitting (LCF) and principal component analysis (PCA) can be used to elucidate the speciation of metals in soils. These techniques in conjunction with *in vitro* bioaccessiblity tests will ensure a more accurate estimation of risks, which will lead to a boost in regulatory and public confidence in risk assessment (Scheckel et al., 2009). However, not much metal speciation research has been done to provide real data to complement *in vitro* bioaccessibility studies.

Accordingly, the overall objective of this thesis is to determine the effect of chemical speciation on the bioaccessiblity of Zn and Pb in spiked and smelter-affected soils. It is hypothesized that readily soluble metal species will contribute more metal ions to bioaccessible metal concentrations than sparingly soluble metal species.

The next chapter of this thesis (Chapter 2) reviews pertinent literature or background materials relevant to the research objectives; this is followed by an investigation of the relationship between soil spiking methods and the chemical speciation of Zn and Pb (Chapter 3). Finally, in Chapter 4, tests are conducted to determine the species of Zn and Pb, identified in Chapter 3, that contribute towards bioaccessible metal concentrations in simulated gastric and duodenal fluids.

2 LITERATURE REVIEW

2.1 Human Health Risk Assessment (HHRA)

Guidelines, established by Health Canada for assessing risks posed to humans by contaminated sites, are designed to ensure that the policy and remedial techniques employed to clean up contaminated sites are consistent (Health Canada, 2004, 2010). The HHRA begins with a Preliminary Quantitative Risk Assessment (PQRA), which uses conservative methods to determine whether a contaminated site poses negligible or acceptable risks to humans. If the risk is acceptable, no significant remedial action is required. Conversely, if the PQRA determines that the risk level is substantial, Site-Specific Risk Assessment (SSRA) is necessary to replace the conservative assumptions made during PQRA with relevant scientific data. Site specific risk assessment provides a more realistic estimation of risks and a firm basis for the selection of remedial techniques. The SSRA is an intensive research process that proceeds in four stages: problem formulation, exposure assessment, toxicity assessment and risk characterization. Data from the exposure estimation and toxicity assessment stages are integrated during risk characterization to quantify the potential risks of contaminants. One critical parameter required for risk characterization is the exposure or dose rate. The dose rate, estimated during exposure assessment, is the amount of a contaminant that comes into contact and taken into the body over a specified period. For systemically acting contaminants like metals, the dose rate is expressed as an internal dose, which is the rate at which a metal is absorbed into the body relative to a receptor's body weight. The internal dose rate for incidentally ingested soils is calculated using the following general equation:

$$Dose\ \left(mg\ kg^{-1}\ day^{-1}\right) = \frac{C_S \times IR_S \times RAF_{GIT} \times ET}{BW} \qquad \text{(Eq. 2.1)}$$

where C_S $(mg\ kg^{-1})$ is the concentration of a contaminant in soil; IR_S $(kg\ day^{-1})$ is the soil ingestion rate; RAF_{GIT} is the relative absorption factor from the GIT; ET is the exposure term; BW (kg) is the body weight (Health Canada, 2010).

The RAF "describes the ratio of the absorbed fraction of a substance from a particular exposure medium relative to the fraction absorbed from the dosing vehicle used in the toxicity study for that substance" (Ruby et al., 1999). That is, for an ingested contaminated soil, the oral bioavailable fraction of the contaminant is essential in estimating the RAF. Oral bioavailability determinations for metal contaminated soils are based on *in vivo* studies, but due to high costs, time constraints and ethical issues, physiologically based *in vitro* digestion models have been developed to determine oral bioaccessibility, which is predictive of a contaminant's oral bioavailability (Ruby et al., 1999; Oomen et al., 2002). *In vitro* digestion models mimic part or all of the human GIT and vary in complexity; the simplest form simulates the gastric pH conditions in the stomach (Oomen et al., 2002). More complex models such as the simulator of the human intestinal microbial ecosystem (SHIME) simulates conditions in the stomach, small intestine, ascending colon, transverse colon and descending colon. The SHIME is dynamic; that is, it mimics the gradual movement of ingested substances through the gut (Williams et al., 2015). Other models simulate movement in the gut by sequential exposure of substances to simulated gastrointestinal conditions; these models are referred to as static (Oomen et al., 2002). Although complex gastrointestinal models simulate more human gut compartments, simpler models like the physiologically based extraction tests (PBET)are convenient to use and can be used to assess the bioaccessibility of a large number of samples. However, because absorption occurs via the intestinal epithelium, simple stomach models may provide bioaccessibility values that are not representative of the absorption site. Also, PBET models do not consider absorption, metabolism, excretion, or sequestration of metals in the gut (Zia et al., 2011). In cases where the principal determiner of bioaccessiblity is pH, simple stomach models simulate bioaccessibility accurately. An evaluation of five *in vitro* digestion models by Oomen et al. (2002) showed that bioaccessibility of Pb increased at low pH and decreased at high pH.

Conditions in the stomach and other parts of the GIT affect the dissolution and subsequent absorption of metals across the intestinal epithelium. However, the solubility of metals from a soil matrix is affected mainly by chemical speciation, which depends on soil properties including soil texture, pH, cation exchange capacity, redox conditions, organic matter content, the presence of anionic species and residence time.

2.2 Speciation of metals in soils

Generally, a species of an element is defined by the chemical and physical form of that element; oxidation state, isotopic composition, coordination with ligands, association with solid phases all contribute to the identification of a species of an element (Reeder et al., 2006; Templeton et al., 2000) . These properties determine the solubility, mobility, fate, and toxicity of elements in the environment and in human organs. The properties that control chemical behavior are determined by processes such as dissolution/precipitation, complexation with ligands, sorption/desorption by solid particles, biotransformation, and reduction/oxidation, as illustrated in Fig. 2.1 (Reeder et al., 2006; Adamo & Zampella, 2008) . These processes are in turn driven by soil properties; for instance, in the soil solution, a metal could exist as a free ion or form different species as a result of hydrolysis and complexation reactions, which are dependent on the pH of the soil solution. Also, the presence of ligands (e.g., PO_4^{3-}, SO_4^{3-}, $A_SO_4^{3-}$) in soil solution promotes the formation of metal-ligand complexes with varying degrees of solubility (Sparks, 2003; Seshadri et al., 2015). In soils with clay minerals that have permanent negative charges, positively charged metal ions (such as Zn^{2+} and Pb^{2+}) are adsorbed onto the charged clay surfaces, reducing the bioaccessibility of the metals. A detailed discussion of how soil properties and processes affect metal speciation is presented below.

2.2.1 Sorption/desorption of metals in soils

Sorption is a generic term used to describe the retention of solutes onto a solid material at the solid-liquid interface, and its is often used when the retention mechanism at the surface is not known (Sparks, 2003; Smith, 1999). Sorption is a crucial chemical process in soils because it determines the fate and mobility of plant nutrients as well as several metal contaminants. Surface complexation and surface precipitation are two major types of sorption processes; the former describes the adsorption reaction between an aqueous chemical species and a functional group at the soil surface, while the latter represents the three dimensional accumulation of an adsorbate (e.g., metal ion) onto a soil surface (Smith, 1999). In soils, surface functional groups can either be inorganic or organic. Inorganic surface functional groups occur at the surfaces of secondary minerals including hydrous oxides, oxides and oxyhydroxides of Fe and

Mn; hydrous oxides of Al and Si, and clay minerals such as kaolinite and smectites. Carboxyl, carbonyl, and phenolic are examples of organic functional groups that occur on the surfaces of humic and fulvic acids in soils. Hydroxyl (OH^-) groups form on metal oxide surfaces when water molecules react with the surface metal ion; this is due to chemisorption (chemical bonding to the surface) and subsequent hydrolysis of the metal oxide surface via ligand exchange (Sparks, 2003; Smith, 1999).

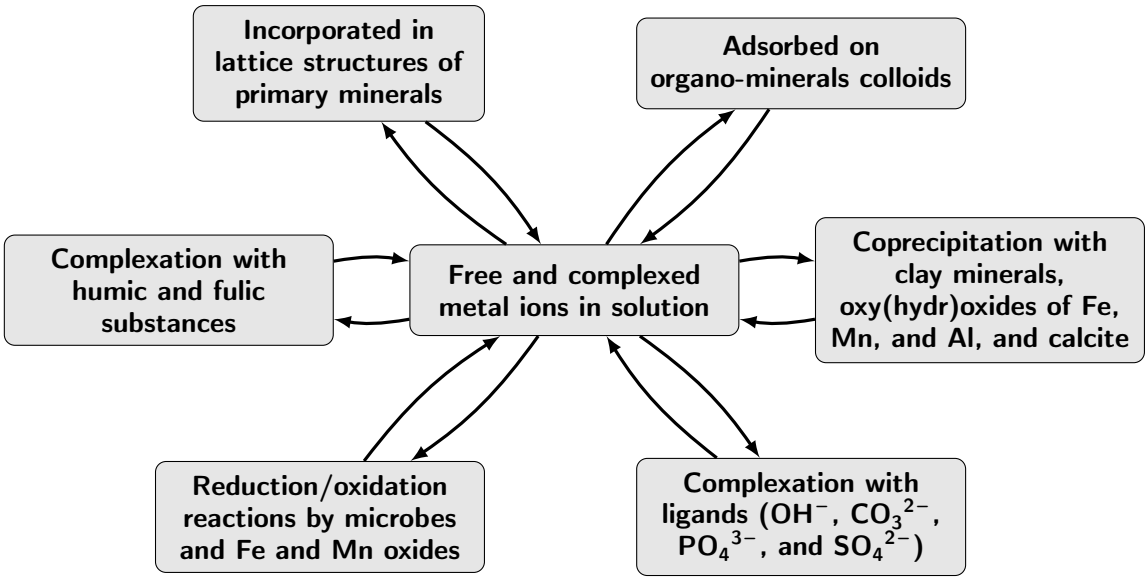

Fig. 2.1: Speciation of metals in soils. Adapted from Adamo et al. (2008)

A surface complex forms when an aqueous metal ion reacts with a surface functional group. The interaction that leads to the formation of surface complexes can either be physical or chemical. Physical interactions involve electrostatic attraction between a hydrated metal ion and a surface functional group of opposite charge. Complexes that form from this process are termed outer-sphere complexes because of the water molecule between the metal ion and the mineral surface. On the other hand, chemical interactions involve the formation of covalent or ionic bonds between the metal ion and the functional group on the mineral surface. The complexes that form as a result of this process are referred to as inner-sphere complexes due to the absence of water molecules between the metal ion and the mineral surface. Surface

complexation reactions are primarily dependent on solution pH and metal ion concentration. For example, employing X-ray absorption fine structure (XAFS), Matocha et al. (2001) found that Pb was held on the surface of birnessite (δ-$MnO_{1.7}$) and manganite (γ-MnOOH) as inner-sphere complexes over a pH range of 1.5-7.5. However, Pb was more strongly bonded to the birnessite than manganite (Matocha et al., 2001). The primary Zn minerals found in most smelter impacted soils are franklinite, sphalerite, and willemite (Manceau et al., 2000; Scheinost et al., 2002; Voegelin et al., 2011). Under acidic soil conditions, these minerals gradually dissolve, releasing Zn^{2+}, which form secondary adsorption species; these include 4-coordinate inner-sphere complexes with aluminum oxides, manganese oxides and ferrihydrite (α-Fe_2O_3). At pH above 7, Zn forms 6-coordinated inner-sphere complexes on goethite (α-FeOOH) (Brown Jr & Parks, 2001; Voegelin et al., 2011).

Phosphate also contributes to the sorption of toxic metals in soils; they form sparingly soluble mineral phases with Pb, Zn, and Cd. For example, under surficial geochemical conditions, Pb reacts with phosphate to form insoluble minerals such as pyromorphite [$Pb_5(PO_4)_3Cl$], fluoropyromorphite [$Pb_5(PO_4)_3F$] and bromopyromorphite [$Pb_5(PO_4)_3Br$] (Traina & Laperche, 1999). Another major factor that contributes to metal sorption in soils is organic matter. Organic substances such as humic and fulvic acids have several functional groups (e.g COOH, OH and C=O); since the point of zero charge (PZC) of these substances is low ($\sim$ pH 3), deprotonation of the functional groups at higher pH values increases their negative charge, and hence their CEC and reactivity with metals. This results in an increase in the adsorption of metal cations (Sparks, 2003). Xia et al. (1997) reported that Cu and Pb form inner-sphere complexes on humic substances at a pH range of 4-6. Using EXAFS, Manceau et al. (1996) found that in the presence of soil humic substances, Pb forms stable complexes with salicylate-type (OH and COOH groups located in ortho position) and catechol-type (two OH groups located in ortho position) functional groups. They concluded that the strength of the complexes accounts for the long residence time of Pb in organic soils (Manceau et al., 1996).

Desorption is the release of adsorbed ions into the soil solution. Metals, whether specifically or non-specifically bound to soil solid particles, can become soluble when

conditions change, especially changes in pH. However, desorption processes have been found to be incomplete; that is, only a fraction of sorbed metals become soluble (Bakes et al., 1995). Several studies have shown that the duration of contact between a sorbed metal and a sorbent (e.g., Fe and Mn oxides) is responsible for the slow rate of metal desorption. Sorption of metals onto mineral surfaces follows a biphasic process: initial rapid reactions, occurring over milliseconds to hours, followed by slow reactions (Sparks, 2003). The subsequent slow reactions may involve the incorporation of metal ions into the lattice structure of soil minerals to compensate for charge imbalances (Backes et al., 1995; Sparks, 2003). With increased contact time, diffusion of metal ions into strongly binding sites (micropores in soil particles and interparticle spaces) has also been suggested to account for the reduction in metal desorption (Hogg et al., 1993).

2.2.2 Precipitation/dissolution of metals in soils

Metal ions form relatively insoluble precipitates with oxyanions (OH^-, ${CO_3}^{2-}$, ${PO_4}^{3-}$ and ${SO_4}^{2-}$) in soil solution and on the surfaces of solid soil particles. As discussed above, metal ions form complexes (outer and/or inner-sphere) on mineral surfaces at low surface sorption densities, but as surface loading increases, metal ions form three-dimensional sorption complexes known as surface precipitates (O'Day, 1999; Ford, Sparks, et al., 2001; Sparks, 2003). Surface precipitation occurs via several mechanisms including 1) reprecipitation of a dissolved mineral surface and an adsorbed metal ion to form what is called a coprecipitate; 2) modification of the solubility product at the mineral-water interface under solution conditions that would, in the absence of a mineral surface, be unsaturated as compared with the solid phase (also known as surface-induced precipitation); 3) nucleation of surface sites under saturated solution conditions, leading to the formation of homogeneous precipitates when monolayer surface coverage is exceeded (Ford & Sparks, 2000; Sparks, 2003).

Coprecipitation depends on the rate of dissolution of a mineral surface. Carbonate, sulfate and calcite minerals have soluble surfaces that dissolve and contribute ions to surface precipitates. Although oxides and silicates are relatively less soluble, studies have shown that these minerals can dissolve and reprecipitate with ions adsorbed from solution (O'Day, 1999). For example, Co(II), Mn(II), Ni(II), and Zn(II) have been

found to form coprecipitates on minerals containing Al(III) and Si(IV) (Sparks, 2003). The dissolution of an Al(III)-containing mineral releases Al, which reacts with an aqueous metal ion to form layered metal-aluminum-hydroxide solid solution. For instance, Zn^{2+} released from the weathering of primary minerals form secondary precipitate species; under acidic conditions, the main Zn precipitate formed is Zn-Al-hydroxide interlayer mineral (HIM). At neutral pH, Zn-Al-layered double hydroxide (LDH) is the dominant Zn precipitate (Nachtegaal et al., 2005; Voegelin et al., 2011). No evidence exists for the formation of a mixed Pb/Al hydroxide phase. This has been attributed to the ionic radii of Pb(II); it is too large to replace Al(III) in the mineral lattice (Sparks, 2003). However, ferric oxyhydroxides have been found to form coprecipitates with Pb(II) at low pH (∼4) (Lu et al., 2011).

Aqueous metal ions also form precipitates with ligands in the soil solution. This occurs at pH 7 and above, where oxyanions (SO_4^{2-}, CO_3^{2-}, PO_4^{3-}, OH^-, AsO_4^{3-}) and Cl^- dominate the soil solution. Metal-ligand complexes may either remain in solution, precipitate or get adsorbed onto mineral surfaces as ternary complexes (Roberts et al., 2005). The formation of ternary complexes is generally described the following equations:

$$\rangle S{-}OH^- + M^{2+} + L^{2-} \longrightarrow \rangle S{-}O{-}M{-}L^{2-} + H^+ \qquad \text{(Eq. 2.2)}$$

$$\rangle S{-}OH^- + M^{2+} + L^{2-} \longrightarrow \rangle S{-}L{-}M + OH^- \qquad \text{(Eq. 2.3)}$$

where $\rangle S-OH$ represents the surface functional group; metal and ligand are represented by M and L, respectively. The solubility of metals held as ternary complexes is lower than that of adsorbed metals (Roberts et al., 2005). Employing infrared spectroscopy and X-ray absorption spectroscopy, Elzinga et al. (2001) found that lead sulphate formed ternary complexes on the surface of FeOOH. Similar complexes were observed between cadmium (Cd) and sulphate on FeOOH by Zhang and Peak (2007).

2.2.3 Reduction/oxidation of metals in soil

Mineral surfaces and soil microbes mediate redox reactions that affect the speciation and solubility of metals. Metals that are often oxidized by microbes include As,

Cr, Hg and Se (Seshadri et al., 2015). Under well-drained conditions, toxic As(III) is oxidized to As(V) by bacteria; As(V) is highly immobile due to its strong affinity for inorganic soil particles (Seshadri et al. 2015). However, when reduced conditions prevail, the mobile and toxic As(III) dominates the soil. Unlike As, the oxidation of Cr(III) to Cr(VI) enhances the mobility and toxicity of Cr. Manganese oxides containing Mn(III/IV) have been found to be the primary oxidizers of Cr in soils and sediments. Conversely, Cr(VI) is reduced to Cr(III) by Fe(II) containing oxides (Sparks, 2003). Manganese oxides (e.g., Mn_3O_4 and MnO_2) may catalyze the oxidation of Co(II), Ni(II), Cu(II) and Pb(II). This involves a process termed disproportionation, where the Mn oxide is simultaneously oxidized and reduced to give Mn^{2+} and MnO_2, leaving vacancies in the Mn oxide structure. Due to the similarities in physical size, Co(II), Ni(II), Cu(II) and Pb(II) fill these vacancies and become incorporated into the Mn oxide structure (Sparks, 2003). Chuan et al. (1996) reported that, under reducing conditions, Zn and Pb bound to oxyhydroxides of Fe and Mn become more soluble due to the dissolution of the oxyhydroxides.

2.3 X-ray Absorption Spectroscopy (XAS)

As discussed earlier, soil properties largely influence the distribution of metal species in soils; these metal species in turn affect metal bioaccessibility, which serves as a conservative estimate for metal bioavailability. Thus, characterizing the distribution of metal species in contaminated soils is key to the accurate estimation of the risks associated with metal contaminated soils. Fortunately, XAS has been established as an effective tool for studying metal speciation in soils (Manceau et al., 2000; Sivry et al., 2010). This molecular scale technique involves directing an X-ray beam of intensity I_0 at an element of interest in a material (in this case a soil sample) of thickness x, as the beam traverse through the soil sample; its intensity drops to I_1 due to absorption by the element of interest. The incident I_0 and transmitted I_1 X-ray intensities are measured as a function of X-ray energy $E(eV)$. The linear absorption coefficient $\mu(E)$ is then determined using the following equation (Rehr & Albers, 2000; Sparks, 2003):

$$\mu(E)x = -\ln \frac{I_0}{I_1} \qquad \text{(Eq. 2.4)}$$

Plotting $\mu(E)$ against X-ray energy $E(eV)$ produces an XAS spectrum as shown in Fig. 2.2. The region, in figure 2.2, characterized by a sharp increase in absorption is known as the edge and it reflects the energy required to excite an inner-shell electron to produce a photoelectron. The absorption edge is unique to each absorbing atom; it is termed K-edge when the core electron is ejected from the 1s core level (Rehr & Albers, 2000). The region of the spectrum that extends to about 30 eV from the absorption edge is the X-ray absorption near edge structure (XANES); this region is diagnostic of the oxidation state of the atom of interest. The oscillations beyond about 30 eV from the edge are the extended X-ray absorption fine structure (EXAFS) (Rehr & Albers, 2000).

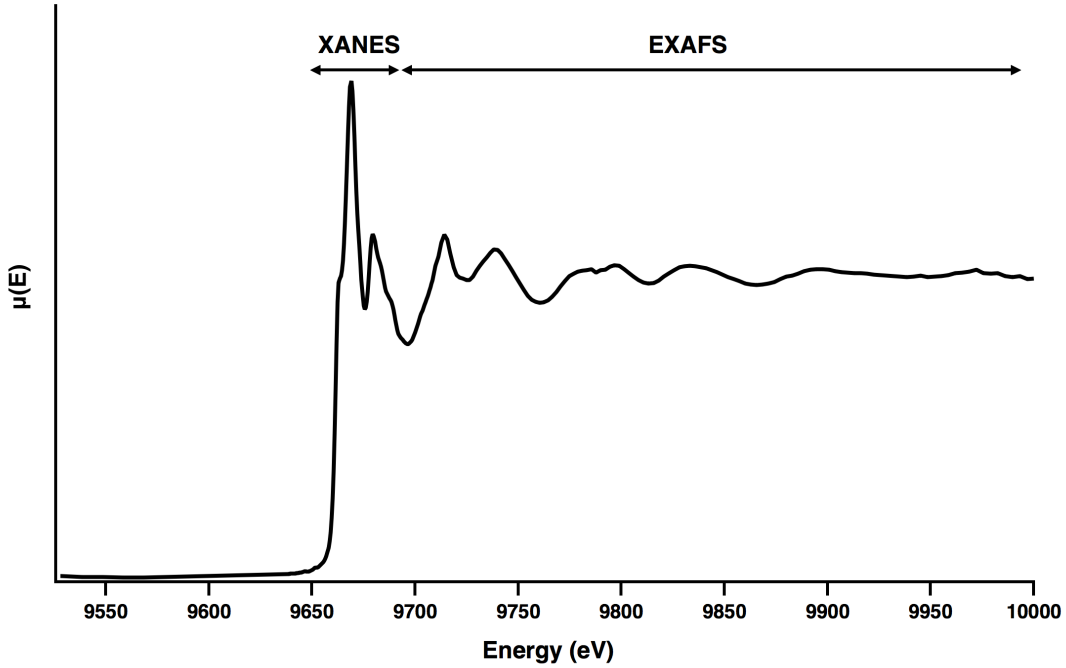

Fig. 2.2: Zn k-edge XAS spectrum, showing the X-ray absorption near edge structure (XANES) and extended X-ray absorption fine structure (EXAFS).

The EXAFS wiggles arise from the interference between the ejected photoelectron wave and backscattered waves from atoms surrounding the absorbing atom (Yano & Yachandra, 2009). For XAS analysis involving a single chemical species, a Fourier transform of the EXAFS oscillations yields structural information, such as bond distances, coordination numbers and neighboring atoms (Rehr & Albers, 2000; Yano & Yachandra, 2009).

However, soils usually contain multiple species of an element, and the XAS spectra collected from scanning a soil sample represents the average contributions from all species present in the sample. This heterogeneity complicates XAS spectra analysis by Fourier transform (Manceau et al., 2000). A more suitable technique used to retrieve species and their relative contributions to multi-species XAS spectra is linear combination fitting (LCF) (Manceau et al., 2000; Jacquat, Voegelin, & Kretzschmar, 2009c; Voegelin et al., 2011; Hamilton et al., 2016a; Hamilton et al., 2016b). It involves using least squares minimization to refine a linear combination of standard spectra to an experimental spectrum, as shown in Fig. 2.3. A good LCF analysis requires a large spectral library of relevant reference compounds (Manceau et al., 2000; Voegelin et al., 2011). However, the results of LCF analysis should not be considered in isolation because there could be multiple combinations of the reference spectra that will satisfactorily fit the experimental spectrum. Uncertainty in LCF results can be reduced by complementing them with relevant information such as the mineralogy and chemical properties of the soil, the total metal content, and knowledge of metal speciation mechanisms. Linear combination fitting has its limitations: it preferentially detects metal species that contain high X-ray scatterers (e.g., Fe and Mn), and it cannot differentiate between adsorption species with similar coordination geometry (Manceau et al., 2000).

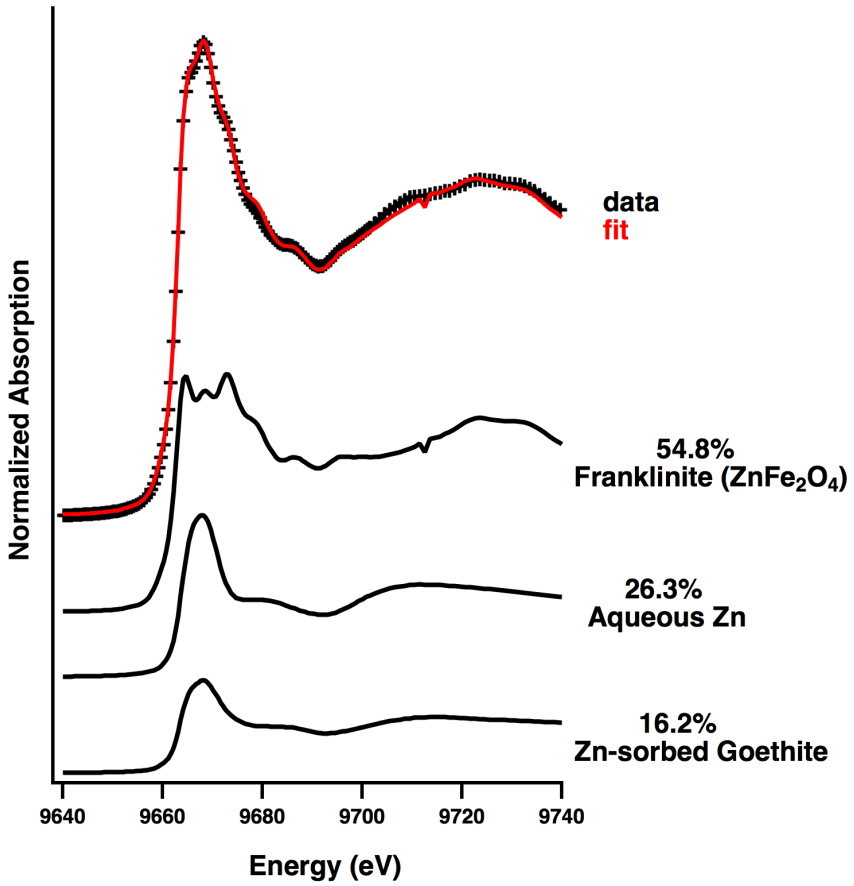

Fig. 2.3: Example of LCF modeling of Zn k-edge XANES spectrum of soil sample (black + symbols). The best fit LCF is shown in red, and the three standard compounds: franklinite, aqueous Zn, and Zn-adsorbed on goethite and their relative contributions to the experimental spectrum are shown below the fit.

2.4 X-ray diffraction (XRD)

X-ray diffraction is a widely used technique in soil science research, and it has been successfully used to determine the atomic structure of crystalline soil inorganic particles (Brown & Brindley, 1980). XRD analysis is based on the fact that crystals are made of small structural units called unite cells, which are arranged in a regular repeated three-dimensional pattern. Also, each unit cell has the same sheet-like arrangement of atoms (Bragg, 1968). When a monochromatic X-ray beam is focused on a crystal, the X-ray waves are diffracted by the sheet of atoms in the crystal. The diffracted waves interfere constructively in some directions and destructively in other directions. For

constructive interference to occur, the path difference for waves diffracted by successive sheets of atoms must be a whole number of wavelengths. The path difference for waves diffracted by successive atomic planes can be determined using the following equation (Bragg, 1968):

$$n\lambda = 2d \sin\theta \qquad \text{(Eq. 2.5)}$$

where n is an integer, λ is the wavelength of the X-ray beam, θ is the glancing angle of the incident X-ray beam, and d, also known as d-spacing, is the distance between successive atomic planes, and it is unique to each crystal or mineral. The diffracted wave patterns are collected, statistically counted and converted to d-spacing, which is used to identify the atomic structure of the crystal. XRD analysis with a single crystal is a more precise technique because of the similar scattering of X-ray beams by unit cells. However, soils contain multiple mineral phases with randomly oriented unit cells. Also, many of these soil minerals occur as aggregates of nanometer-sized particles (Manceau et al., 2002). Thus, it is almost impossible to study soil minerals using single crystal diffraction. Instead, the powder diffraction technique is used; this is made possible by synchrotron produced X-rays. Synchrotron produced X-rays are highly collimated; this allows lateral resolution of the glancing incident beam, which reduces the heterogeneity in powder samples. Besides, the high intensity of the synchrotron beam affords the collection of diffraction patterns with great counting statistics (Manceau et al., 2002).

3 EVALUATION OF SOIL SPIKING METHODS

3.1 Preface

Toxicity and risk assessment studies of metal contaminated soils provide vital information for the formulation of regulations and policies. The assessment of the potential toxicity and risks of metals in soils typically requires the addition of metal salts to uncontaminated soils. This soil spiking method fails to mimic field contaminated soils with regards to metal loadings and metal speciation. Spiking soils with metal salts is likely to alter the pH and EC of the soils, and may result in the formation of metal complexes that either enhance or inhibit metal bioavailability, which in turn affects toxicity. In this chapter, two alternative approaches (annealed metal and metal oxide) to spiking soils are compared with the widely used metal salt spiking method. The speciation results from this chapter will form the basis for the next chapter (Chapter 4), where the effect of metal speciation on bioaccessibility would be studied to determine the metal species that contribute to bioaccessible metal concentrations in simulated gastric and duodenal fluids.

This chapter will be published in a peer reviewed journal. The following people assisted with parts of the experiments conducted in this chapter:

Determination of physical and chemical properties of the soils - Mark Cousins, Kayode Jegede, and Fred Awuah
Collection and analysis of Zn XANES data - Jordan Hamilton

3.2 Abstract

Soil toxicity and risk assessment research usually involve the addition of metals to uncontaminated soils. The common method employed by researchers involve adding metal salts to soils and leaching with artificial rainwater to remove the salts. This method not only fails to mimic field conditions, it may produce artifacts that alter soil chemical properties. As a result, this study assessed the metal salt spiking method and two alternative methods (synthetic or annealed minerals and metal oxides) that make use of solid state metals. The objective was to determine the method that best mimicked smelter-affected Zn speciation and Zn, Pb, and Ni concentrations.

Three different soils with low metal loadings were spiked with three metal mixtures that differed in metal concentrations. The metal mixtures comprised Zn, Pb, Ni, Cu, and Co; the concentration of these metals were derived from smelter-affected soils from Flin Flon, MB, Port Colborne and Sudbury, ON. Thirty days after spiking, the concentrations of Zn, Pb and Ni were determined using X-ray fluorescence (XRF); X-ray absorption near edge structure (XANES) was used to characterize Zn speciation in the spiked soils.

Speciation of Zn was found to depend on spiking method and soil properties, especially pH. Each spiking method produced between 1-3 Zn species that occur in smelter-affected soils. Comparatively, the metal-salt spiking method significantly failed to replicate the environmentally relevant Zn and Ni concentrations. Also, it was found to have several disadvantages that may present serious challenges to toxicity and risk assessment research. At neutral to alkaline pH, metal oxides are sparingly soluble, while the synthetic mineral (franklinite) is resistant to weathering even at low pH. It is therefore suggested that the chemical properties of soils should be taken into account when selecting a spiking method.

3.3 Introduction

Anthropogenic activities, especially metal smelting, are responsible for elevated concentrations of metals in soils (Reeder et al., 2006) . Typically, smelter-affected soils contain more than one potentially toxic metal at elevated levels. Soils in Flin Flon, MB have been found to contain a mixture of As, Cd, Cu, Hg, Pb, and Zn; this was due to decades of base-metal mining and smelting by Hudson Bay Mining and Smelting Company Limited (McMartin et al., 2009). At Port Colborne, ON, the operation of a Ni refinery from 1918 to 1995 resulted in elevated levels of As, Co, Cu and Ni in nearby soils (Dan et al., 2008); and in Sudbury, ON, nickel-copper mining and smelting has lead to the high concentrations of Cu, Zn, Ni, Pb, Cd and As in nearby soils (Sudbury Smelter Business Unit and Falconbridge, ON, 2004). Despite the fact that contaminated soils comprise of more than one toxic metal, current scientific data guiding policy and risk assessment of metal contaminated sites are based on research carried out on individual metals.

Studies, such as phytotoxicity, microbial toxicity and bioavailability studies, provide information for formulating regulatory guidelines for metal contaminated soils. These studies sometimes require mimicking conditions in smelter-affected soils via the addition of metals to uncontaminated soils, usually in increasing metal concentrations. Single metal ecotoxicological experiments involve the exposure of a specific metal at different concentrations to soil microbes and/or plants; in HHRA, it includes the determination of the bioaccessible metal concentration of a given metal. On the other hand, mixture experiments, which are more representative of field conditions, comprise two or more metals. The environmental relevance of such studies depends on (i) whether the spiked soils contain metal(s) at environmentally-relevant concentrations, and (ii) whether the metal species in the spiked soils represent those found in actual field contaminated soils.

Currently, the most commonly used soil spiking method involves adding metal-salts to soils and then leaching with artificial rainwater to reduce the high electrical conductivity (EC) produced by the salts (Broos et al., 2007; Mertens et al., 2009; Ruyters et al., 2009). One major problem with this method is the reduction in metal concentrations after leaching. Thus, the environmentally-relevant metal concentrations cannot

be maintained in the soils using this approach. This constraint led to formulating alternative spiking methods involving solid state metal additions (metal oxide and synthetic metal bearing minerals). Since leaching is not required of the oxide spiking method, the desired metal concentrations can be maintained; however, the second condition may not be fulfilled since metal oxide is just one of many metal species that may be present in field contaminated soils. As mentioned earlier, most metal contaminated soils are a result of smelting activities; the smelting process can be replicated in the lab to produce synthetic mineral species that occur in smelter-affected soils. The synthetic minerals or annealed metals can then be added to soils. This approach may ensure that the environmentally relevant metal concentrations and species are maintained and present in the spiked soils.

The objective of this study was to evaluate the two alternative spiking methods (metal oxides and annealed metals), and compare them to the widely-used method (metal-salts) to determine which is more appropriate for risk assessment and soil toxicological research. For this study, it was hypothesized that the annealed metals will produce metal species that occur in smelter-affected soils and also allow soils to be spiked at environmentally relevant concentrations. A mixture of metals [lead (Pb), zinc (Zn), and nickel (Ni)] was used in this study.

3.4 Materials and Methods

3.4.1 Soil samples

Three soils with relatively low metal loadings were used in this study: 3.22 and WTRS soils from Flin Flon, Manitoba, and UBC soil from Iqaluit, Nunavut. Soil samples were collected at a depth of 15 cm and air dried for 48 hours. The pH of the soils was determined using $CaCl_2$ extraction (1 g soil and 5 mL 0.01 M $CaCl_2$) (Environment Canada, 2007). Organic carbon (OC) content was determined using a CNS analyzer (Leco SC-623); soils were treated with HCl to remove inorganic carbon before combustion. Effective cation exchange capacity (eCEC) was determined by $BaCl_2$ extraction (Belanger, Pare, & Hendershot, 2012). Background Zn, Pb, and Ni concentrations were determined in each soil by X-ray fluorescence (XRF) spectroscopy (Thermo Scientific ARL OPTIM' X X-ray analyzer). The mineralogy and determined chemical properties of

Table 3.1: Mineralogy and chemical properties of reference soils.

Soil ID	pH	Organic C	eCEC	Clay content	Zn	Pb	Minerals
		- - g kg^{-1} - -	- - cmol kg^{-1} - -	- - g kg^{-1} - -	- - - mg kg^{-1} - - -		
3.22	3.4	17	32.6	45	1190	601	Quartz Albite Orthoclase
WTRS	4.6	25	37	110	1120	146	Quartz Albite Magnetite Muscovite
UBC	5.6	12	33.3	24	57	0	Quartz Albite Faujasite

the test soils are shown in Table 3.1. Each soil was spiked using the above-mentioned methods: metal nitrates and leaching, metal oxides and annealed metals. Also, each spiking method consisted of three different mixture concentrations (target concentrations) based on the average levels of Zn, Pb, and Ni in contaminated soils from Flin Flon, Port Colborne, and Sudbury. The target concentrations from the three sites are shown in Table 3.2. In all, the study involved 27 spiked soil samples.

3.4.2 Spiking with metal nitrates and leaching

Stock 1 L solutions of each metal were prepared using metal nitrates from Sigma-Aldrich: $Pb(NO_3)_2 \cdot 6H_2O$, $Ni(NO_3)_2 \cdot 6H_2O$, and $Zn(NO_3)_2 \cdot 6H_2O$. Taking into account the field capacity (FC) of each soil, the metal stock solutions were pipetted into the soils at the required ratios and thoroughly mixed. The electrical conductivity (EC) of the spiked soils were then adjusted to that of the controls (un-spiked soils) by leaching with artificial rainwater (Li et al., 2010). Afterwards, deionized water was added to the soils at 50% FC at two weeks intervals for a 30 days. All soils were incubated in a phytotron (temperature 20-23 °C) during the one month period to simulated drying and wetting field conditions.

3.4.3 Spiking with synthetic minerals

Synthetic minerals were prepared using a co-precipitation method. Based on concentrations determined in smelter-affected soils from Flin Flon, Port Colborne and Sudbury, aqueous metal nitrates of Zn, Pb, and Ni were mixed with aqueous Fe^{2+} [$Fe(NO_3)_2 \cdot 6H_2O$] nitrate (Fe made up 70% of total metal weight). The pH of all 3 mixtures was then raised to neutral with 12 M NH_4OH. Afterwards, the mixtures were placed in a horizontal shaker for 24 hours and then centrifuged at 2000g for 30 minutes. The precipitates were dried in a fume-hood for 3 days. Subsequently, the dried precipitates were charred in a muffle furnace at 500 °C for 10 minutes. The charred materials (annealed metals) were ground, weighed and thoroughly mixed with the soils. The spiked soils were watered at two weeks intervals for 30 days using deionized water at 50% field capacity. All soils were incubated in a phytotron (temperature 20-23 °C) during the 30 days period to simulated drying and wetting field conditions.

3.4.4 Spiking with metal oxides

Metal oxides (PbO_2, NiO_2, and ZnO_2) from Sigma-Aldrich were used for this spiking method. Before spiking, the oxides were placed in a desiccator together with concentrated HCl to rid the oxides of inorganic carbon. Afterwards, the oxides were ground, weighed and thoroughly mixed with the soils. Deionized water was added to the soils at 50% FC at two weeks intervals for 30 days. All soils were incubated in a phytotron (temperature 20-23 °C) during the one month period to simulated drying and wetting field conditions.

Table 3.2: Source and concentration of metal mixtures.

	Mixture composition		
Mixture source	Zinc	Lead	Nickel
	- - - - - - - - - - - - mg kg^{-1} - - - - - - - -		
Flin Flon	4489.8	417.2	19.3
Port Colborne	366.3	113.9	3201.3
Sudbury	2176.2	5049.0	536.4

3.4.5 X-ray diffraction (XRD) analysis

X-ray powder diffraction analysis was performed at the Canadian Macromolecular Crystallography Facility bending magnet (CMCF-BM) (08B1-1) beamline located at the Canadian Light Source (CLS), Saskatoon. X-ray diffraction data were collected at an energy of 18 keV and a wavelength of 0.68888 Å. Diffraction patterns were collected using a high-resolution, widearea detector (Rayonix MX300-HE). The uncontaminated soil samples and annealed materials were ground using mortar and pestle, and then loaded into polyimide tubes for XRD analysis. Data processing was completed using the GSAS-II software package (Toby & Von Dreele, 2013), integrating over the range from 2 to 37 degrees 2θ (Å). Phase identification was performed using the X' Pert Highscore Plus module.

3.4.6 X-ray fluorescence (XRF) analysis

Both background metal concentration and total metal concentration after spiking were determined using a Thermo Scientific ARL OPTIMA' X X-ray analyzer, which converts counts per second to mg kg^{-1}. This method was used because it is non-destructive and has a low error margin of ± 10%. All soil samples were ground to uniform fine particle size and loaded into XRF sample holders for analysis. Metal concentration data was then extracted using an OptiQuant software.

3.4.7 X-ray absorption spectroscopy (XAS) analysis

X-ray absorption near edge structure (XANES) analysis was performed on spiked soils. For the Flin Flon mixture spiked soils, Zn K-edge (9659 eV) spectra were collected at the Hard X-ray Microanalysis (HXMA) beamline at the CLS. The CLS storage ring operated at 2.9 GeV and the beam current varied between 150-250 mA. The beamline monochromator consisted of a Si-220 crystal adjusted to a spot size of 0.5-1.5×0.7-2.5 mm. The monochromator was detuned by 50% to reduce higher harmonics and calibrated to the first inflection point of the K-edge Zn reference foil of 9659 eV. The XANES spectra for all samples were collected in fluorescence mode at ambient temperature with a 32-element Ge detector (Canberra); a Cu-6 filter and Soller slits were placed between the sample and detector to reduce scattering and unwanted fluorescence from other elements. Aluminum foil was also placed over the 32-element de-

tector to improve signal to noise by preferentially reducing Fe fluorescence from samples. For each sample, 2-3 scans were collected, depending on metal concentration. All XANES spectra were analyzed with ATHENA (Ravel & Newville, 2005). Briefly, for each scan, the background was subtracted and calibrated to the Zn reference foil (9659 eV). Scans were smoothed when necessary and the absorption edge was set at the zero crossing of the second derivative. Individual scans of each sample were then merged. Using a spectral library of Zn standard compounds prepared by (Hamilton et al., 2016a), the semi-quantitative approach of linear combination fitting was used to retrieve the contribution of each standard spectrum to each sample spectrum. The fitting range for XANES data was between 9640-9740 eV.

3.5 Results and Discussion

3.5.1 Phase identification of synthetic minerals

The synthetic minerals, prepared via the co-precipitation of aqueous metal and Fe^{2+} nitrates, and heat treatment of the precipitates at 500 °C, were identified using synchrotron-based X-ray powder diffraction. The diffraction pattern of the Flin Flon mixture sample (Fig. 3.1a) shows the presence of magnetite and franklinite diffraction peaks, indicating the presence of magnetite and franklinite spinel minerals in this sample. However, there is little difference between some of the diffraction peaks of magnetite and franklinite due to similarities in their crystal structure. Fig. 3.1b shows the diffraction pattern of the Port Colborne mixture sample. Magnetite and trevorite (Ni-rich) diffraction peaks were found in the pattern, suggesting the presence of magnetite and trevorite (Ni-rich) spinel minerals. Difficulty in differentiating magnetite peaks from trevorite (Ni-rich) peaks is due to similarities in the cubic crystal structure of these minerals. Magnetite and hydrocerussite diffraction peaks were found in the diffraction pattern of the Sudbury mixture sample (Fig. 3.1c). The raised baseline at the lower angle of the diffraction pattern suggests the presence of non-crystalline phases of hydrocerussite in this sample. Hydrocerussite is the only non-spinel mineral formed from the annealing process; this is due to the inability of Pb to substitute for Fe in magnetite mineral. Franklinite is one of the common Zn minerals found in smelter-affected soils (Manceau et al., 2000; Scheinost et al., 2002; Voegelin et al., 2011; Hamilton et al., 2016a). At the smelter-affected site at Flin Flon, MB, Hamilton

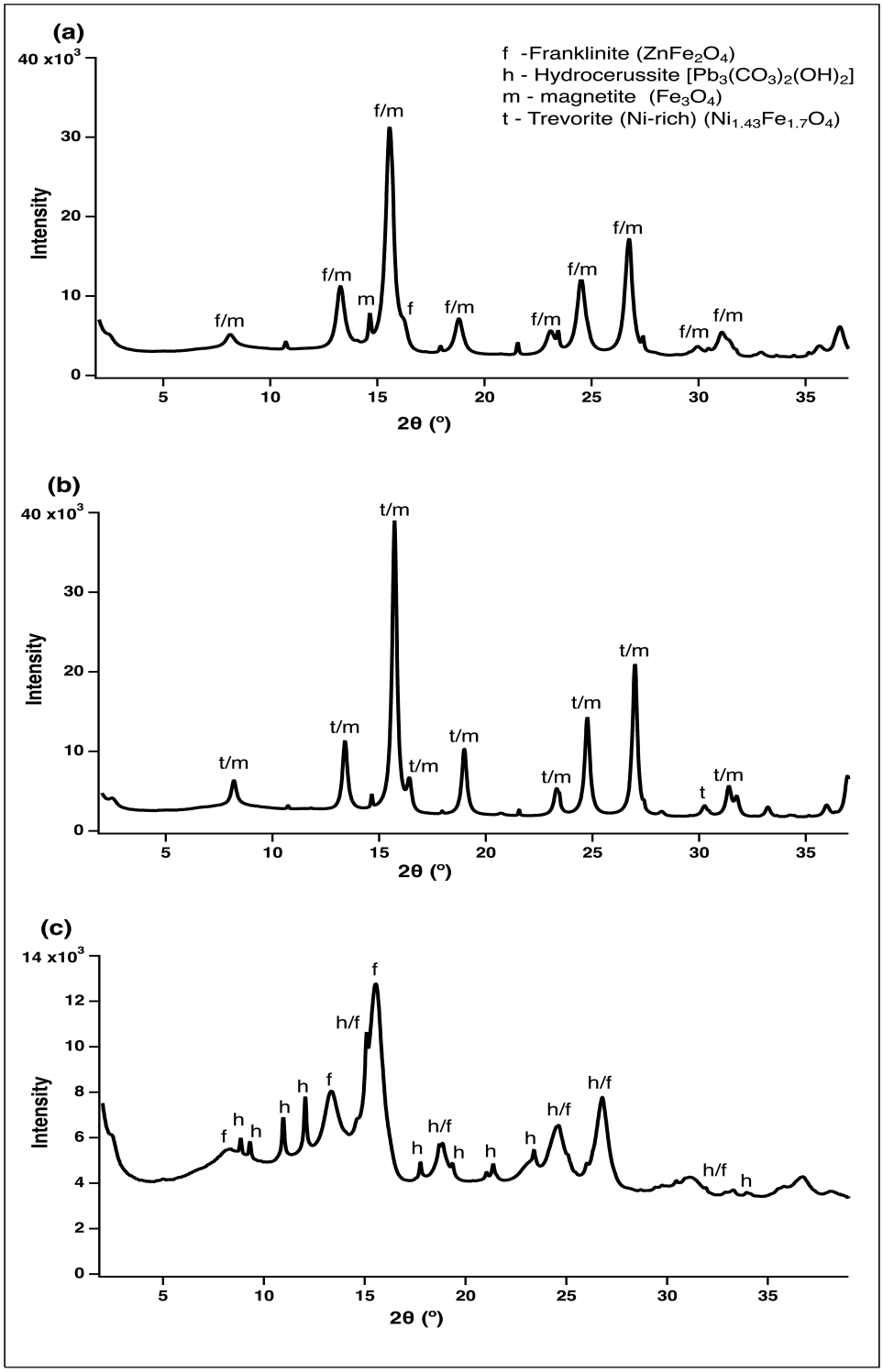

Fig. 3.1: X-ray powder diffraction pattern of synthetic minerals; (a), (b), and (c) represent synthetic minerals produced from Flin Flon, Port Colborne, and Sudbury mixtures, respectively.

et al., (2016) found that franklinite was the main Zn mineral in the contaminated soils, occurring in high concentrations regardless of distance from the smelter. Hydrocerussite is a secondary Pb mineral that occurs in smelter-affected soils with high carbonate content; however, its contribution to the total Pb concentration is often low (Ostergren et al., 1999; Morin et al., 1999).

3.5.2 Total Zn, Pb and Ni concentrations in spiked soils

The first objective of this study was to determine the spiking method that mimics environmentally relevant Zn, Pb, and Ni concentrations derived from smelter-affected soils at Flin Flon, Port Colborne, and Sudbury. Fig. 3.4 and 3.5 show the background corrected Zn and Ni concentrations in the spiked soils compared to their target concentrations. For soils spiked with Zn and Ni nitrates and later leached with artificial rainwater, background corrected Zn and Ni concentrations were far below their target concentrations (for all three mixtures). This is probably due to the combined effects of soil properties and leaching. All three soils are acidic hence the adsorption sites are dominated by H^+ ions, leaving Zn and Ni in the soil solution; since Zn and Ni do not strongly bond with organic matter, they are readily transported out of the soils by advection. Conversely, background corrected Pb concentrations were either at or above the target levels (Fig. 3.6), suggesting that leaching did not affect Pb concentrations. The persistence of Pb may be due to the formation of inner-sphere complexes with organic matter (Xia et al., 1999). Contrary to the nitrate spiked soils, background corrected Zn and Ni concentrations in the oxide spiked soils were above their target concentrations (Fig. 3.3 and 3.4). The difference between the background corrected and target concentrations, for the oxide spiked soils, was not as large as that observed for the nitrate spiked soils. Background corrected Pb concentrations in the oxide spiked 3.22 soil were above the Pb target concentration for the Flin Flon and Port Colborne mixtures, but below the target concentration for the Sudbury mixture (Fig. 3.6). In the oxide spiked WTRS and UBC soils, background corrected Pb concentrations for Flin Flon and Sudbury mixtures were below the Pb target concentration; for the Port Colborne mixture, the background corrected and target concentrations were almost the same (Fig. 3.6). Except for the annealed spiked 3.22 and WTRS soils (Flin Flon mixture), the background corrected Zn, Pb, and Ni concentrations in the annealed spiked soils were either slightly above or below their target levels (Fig. 3.4, 3.5, and 3.6).

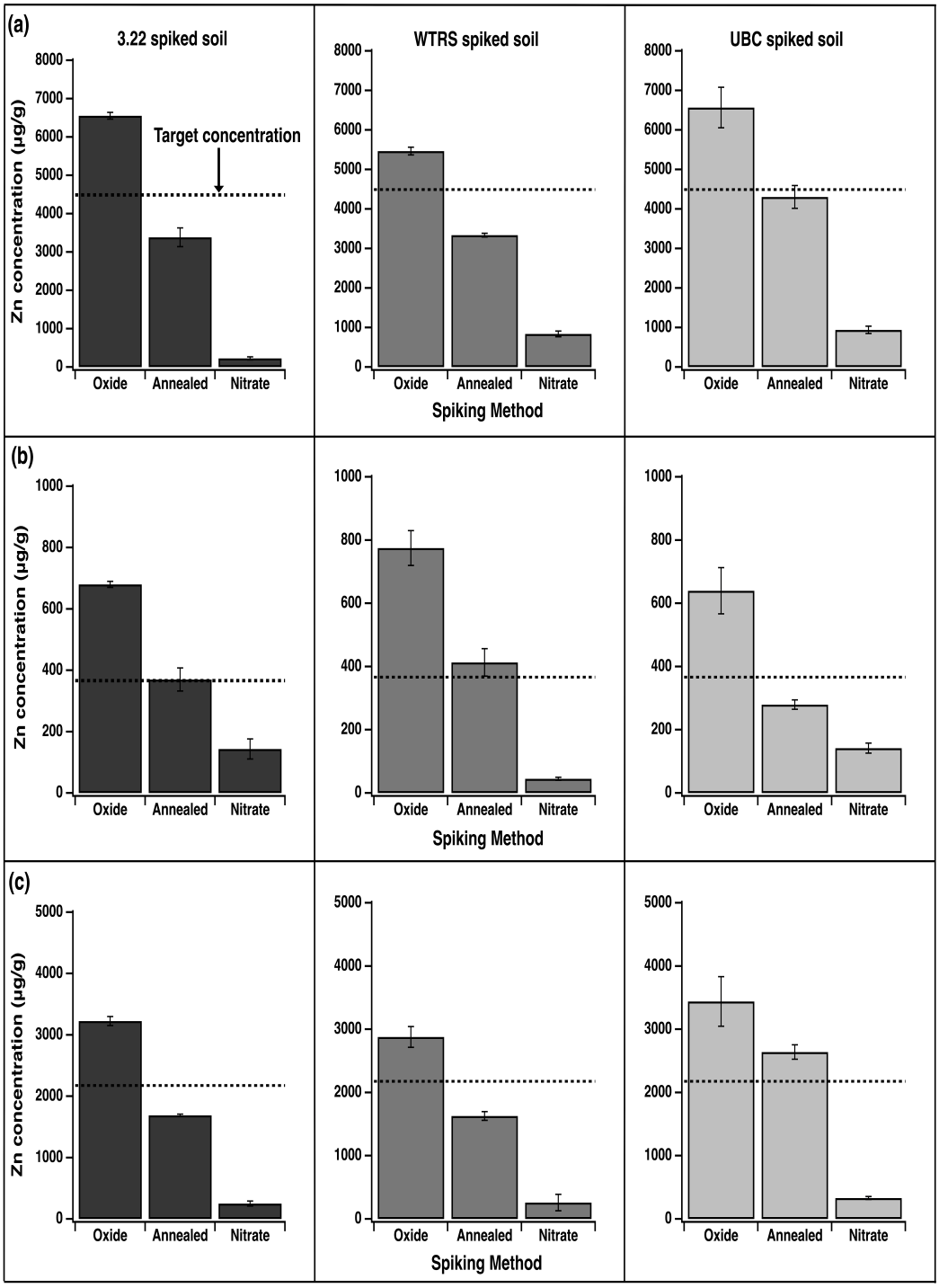

Fig. 3.2: Background corrected total Zn concentration in 3.22, WTRS, and UBC spiked soils; (a), (b), and (c) represent Flin Flon, Port Colborne and Sudbury mixtures, respectively. The target concentrations, which the spiking methods were expected to replicate, were derived from Flin Flon, Port Colborne, and Sudbury smelter-affected soils.

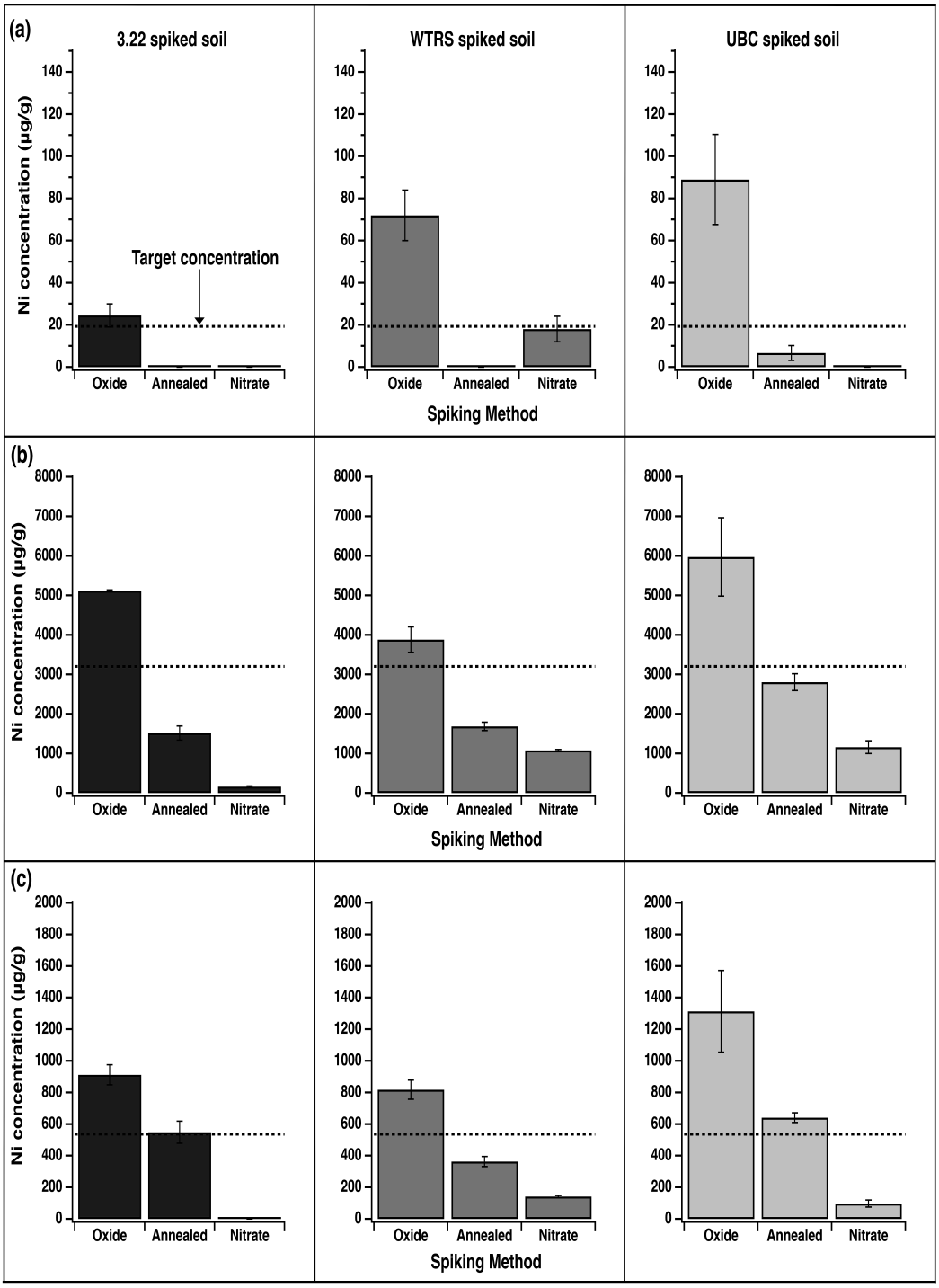

Fig. 3.3: Background corrected total Ni concentration in 3.22, WTRS, and UBC spiked soils; (a), (b), and (c) represent Flin Flon, Port Colborne and Sudbury mixtures, respectively. The target concentrations, which the spiking methods were expected to replicate, were derived from Flin Flon, Port Colborne, and Sudbury smelter-affected soils.

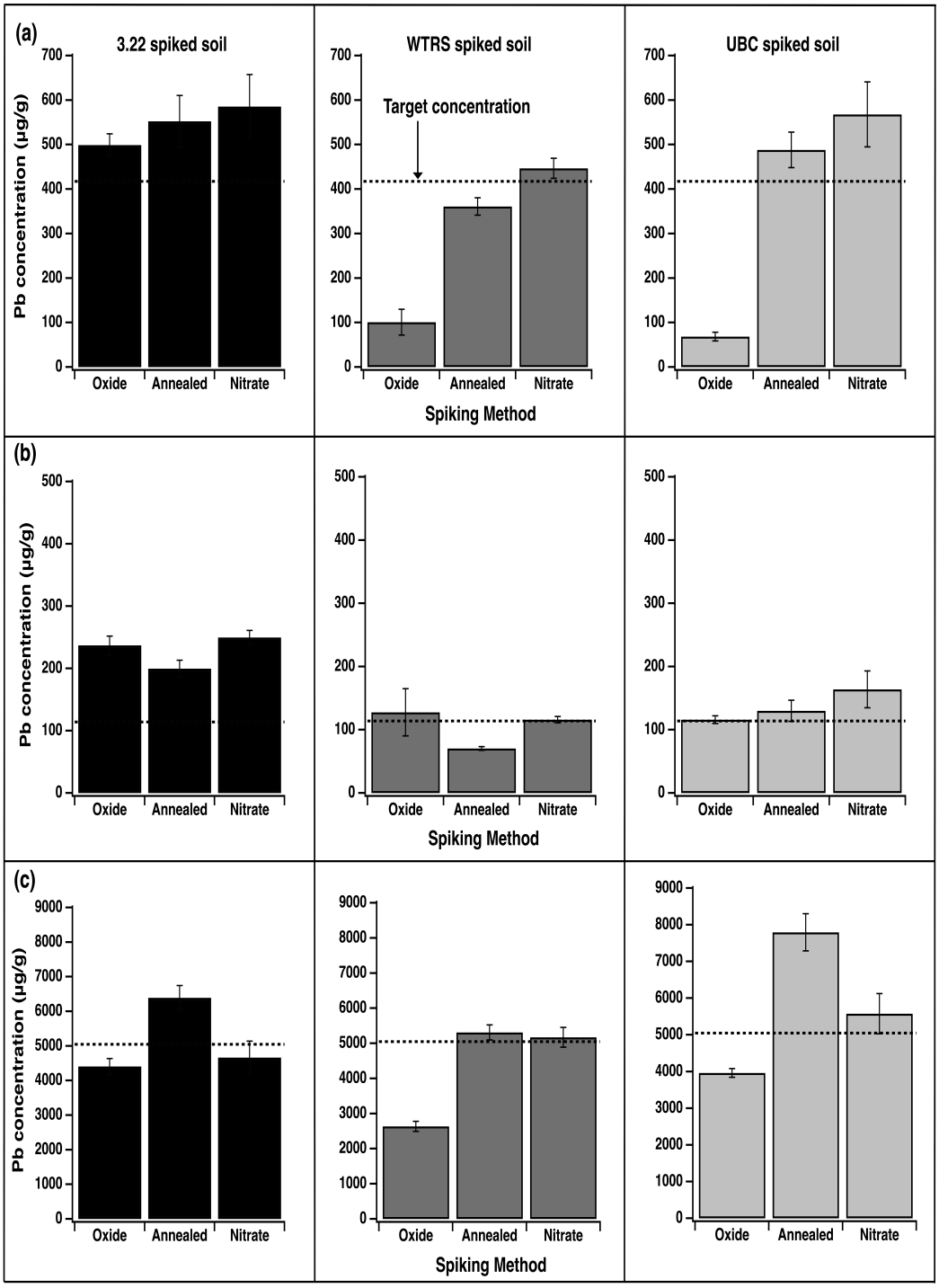

Fig. 3.4: Background corrected total Ni concentration in 3.22, WTRS, and UBC spiked soils; (a), (b), and (c) represent Flin Flon, Port Colborne and Sudbury mixtures, respectively. The target concentrations, which the spiking methods were expected to replicate, were derived from Flin Flon, Port Colborne, and Sudbury smelter-affected soils.

3.5.3 Zn speciation in spiked soils

The speciation of all the metals (Zn, Pb, and Ni) in each of the mixtures was beyond the scope of this study. Speciation of Zn in the spiked soils was investigated because of the availability of a spectra library of Zn standard compounds. Besides, Zn is the dominant metal in the smelter-affected soils at Flin Flon, and its speciation at this site has been characterized in a previous study by a member of the research team (Hamilton et al., 2016a; Hamilton et al., 2016b). For these reasons, Zn K-edge XANES spectra were collected from only soils spiked with the Flin Flon mixture (nine spiked soil samples). Bulk Zn K-edge XANES spectra with corresponding LCF spectra for the nine spiked soils are plotted in Fig. 3.7. The XANES spectra are visually different, indicating that speciation of Zn in these samples is different. The results of the LCF along with the total Zn concentrations in the spiked soils are shown in Table 3.3. Regardless of spiking method, 3.22 spiked soils were found to contain franklinite, sphalerite, and outer-sphere/aqueous Zn; however, the relative abundance of these Zn species differed between the spiking methods. The presence of franklinite in both the nitrate and oxide spiked soils suggests that the 3.22 soil had a significant background franklinite component, which is about the fraction (23%) in the oxide spiked soil. The presence of synthetic franklinite in the annealed material accounts for the high relative abundance (67%) of franklinite in the annealed spiked 3.22 soil. For the nitrate spiked soil, leaching of nitrate salts inadvertently leached soluble Zn species, resulting in a low total Zn concentration, but franklinite is resistant to dissolution even at low soil pH and hence its fraction increased as the soluble Zn components decreased. The relatively low fraction (4%) of sphalerite in the nitrate spiked soil can be partly attributed to leaching. Sphalerite is known to readily dissolve under acidic conditions (Acero et al., 2007), the 3.22 soil is highly acidic (pH 3.4); consequently, saturating the soil with artificial rainwater increased the rate of sphalerite dissolution. ZnO was the only species unique to the oxide spiked 3.22 soil; Its low relative abundance (25%) may be due to its susceptibility to weathering at low soil pHs (Voegelin et al., 2011). Compared to the annealed and nitrate spiked soils, the release of Zn^{2+} from the dissolution of ZnO increased the fraction of outer-sphere Zn in the oxide spiked soil. The XANES spectrum from the annealed spiked WTRS soil was adequately reproduced by a linear combination of 55% franklinite, 16% Zn adsorbed on goethite and 26% outer-sphere/aqueous Zn, leaving only 3% of the spectrum unaccounted for (Table 3.3).

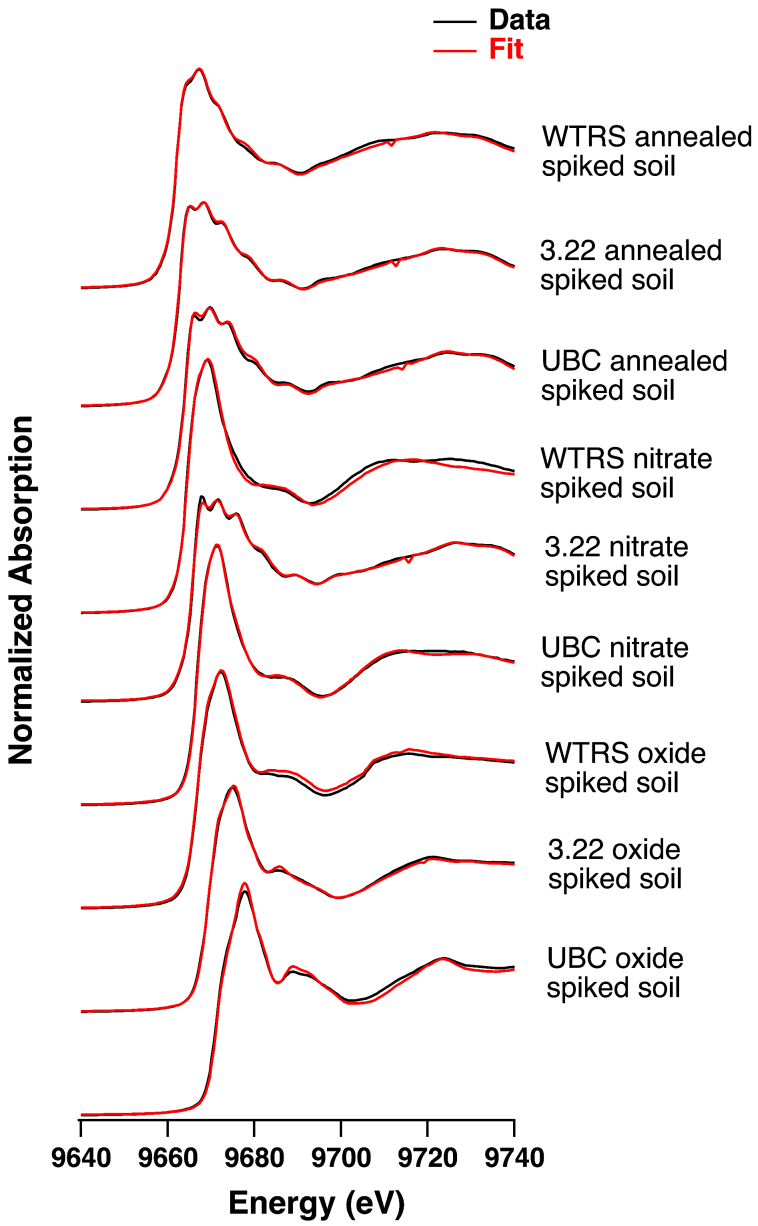

Fig. 3.5: Bulk Zn K-edge XANES spectra (black lines) and linear combination fits (LCF) (red lines) for 3.22, WTRS, and UBC spiked (annealed, oxide and nitrate) soil samples. Zn K-edge XANES spectra were collected from soils spiked with Flin Flon mixture. LCF results are provided in Table 3.3.

Table 3.3: Total Zn concentrations and Linear Combination fits of the XANES from 3.22, WTRS and UBC spiked soils.

								Zn - Sorbed		
ID	Total Zn[†]	Franklinite ($ZnFe_2O_3$)	Sphalerite (ZnS)	Zn-Al-LDH[‡]	ZnO	$ZnCO_3$	Zn-HIM[§]	Goethite (FeOOH)	Outer-sphere/ $Zn^{2+}_{(aq)}$	Reduced χ^2
	- - mg/kg - -	- %[¶] -								
3.22 Annealed	5810	67	6	-	-	-	-	-	25	6.5×10^{-5}
3.22 Nitrate	1690	74	4	-	-	-	-	-	20	1.6×10^{-4}
3.22 Oxide	7770	23	11	-	25	-	-	-	39	1.1×10^{-4}
WTRS Annealed	4420	55	-	-	-	-	-	16	26	1.4×10^{-4}
WTRS Nitrate	1280	-	-	-	-	-	-	96	-	3.7×10^{-4}
WTRS Oxide	6680	-	-	35	16	-	-	48	-	4.3×10^{-4}
UBC Annealed	3800	77	-	-	-	-	-	-	21	1.9×10^{-4}
UBC Nitrate	846	-	-	-	-	46	24	-	28	1.2×10^{-4}
UBC Oxide	5870	-	-	-	53	43	-	-	-	1.4×10^{-4}

[†] Total Zn concentration measured with X-ray fluorescence
[‡] Zinc aluminum layered double hydroxide
[§] Hydroxy interlayered mineral
[¶] Relative contribution to XANES spectra

The similarity between the soil spectrum and LCF model (Fig. 3.7) coupled with the fact that individual components add up to approximately 97% suffice to have high confidence in the LCF result. Unlike the annealed spiked 3.22 soil, all of the franklinite detected in the annealed spiked WRTS soil came from the annealed material because no franklinite component was found in the nitrate and oxide spiked WTRS soils (Table 3.3). Plausible explanations for the presence of Zn adsorbed on goethite, and outer-sphere/aqueous Zn in the annealed spiked WTRS soil are (i) since Zn sorbed on goethite is also present in the nitrate and oxide spiked soils, it represents the background Zn fraction; (ii) the high acidity (pH 4.6) of the WTRS soil may have caused a partial release of Zn^{2+} from franklinite into the soil; subsequently, the released Zn^{2+} was adsorbed onto the surface of goethite. Besides 48% Zn sorbed on goethite, the oxide spiked WTRS soil was found to contain 16% ZnO and 35% Zn-aluminum layered double hydroxide (Zn-Al LDH). The formation of Zn-Al LDH is consistent with results reported by Voegelin et al. (2002 & 2011). After spiking four soils, having pH ranging from 4.2-7.7, with ZnO, Voegelin and fellow researchers found the formation of Zn-Al LDH in all four soils; the relative abundance of Zn-Al LDH, however increased as pH increased (Voegelin et al., 2011). Previous studies by Jacquat et al. (2009) showed that Zn-LDH forms only in slightly acidic to alkaline soils with high Zn concentrations. However, Voegelin and team members posited that limited advective solute flow caused a rise in the pH and Zn loading in the immediate vicinity of the dissolving ZnO particles, leading to the precipitation of Zn-Al LDH in the low pH soils (Voegelin et al., 2011). This is probably what happened in the oxide spiked WTRS soil, which, together with all the spiked soils, was kept in a container that limited advective solute transport. The best LCF for the annealed spiked UBC soil spectrum was obtained by a combination of 77% franklinite and 21% outer-sphere complexed Zn (Table 3.3). Again, the presence of franklinite in this sample was expected since the XRD analysis confirmed that the annealed material contained the Zn-bearing mineral. In the nitrate and oxide spiked UBC soils, the LCF suggested the presence of 46% and 43% $ZnCO_3$, respectively (Table 3.3). In addition to $ZnCO_3$, 53% of ZnO was present in the oxide spiked UBC soil. Other Zn species found in the nitrate spiked UBC soil are outer-sphere complexed Zn (27%) and Zn incorporated into a hydroxy interlayered mineral (Zn-HIM) (24%). The formation of Zn-HIM is consistent with previous studies that found the formation of Zn-HIM in contaminated (Scheinost et al., 2002; Jacquat

et al., 2009b) and uncontaminated (Manceau et al., 2004) soils with low Zn loadings. A hydroxy interlayered mineral (HIM) is a phyllosilicate with hydroxy-polymers in its interlayer, and in acidic soils, the main interlayer component is dioctahedral hydroxy-Al (Jacquat et al., 2009b). At low soil Zn concentrations, Zn^{2+} is specifically sorbed to the hydroxy-Al polymers within the HIM; consequently, Zn-HIM is sparingly soluble even under acidic soil conditions (Jacquat et al., 2009b).

3.5.4 Implications for risk assessment and soil toxicity studies

The results showed that Zn speciation differed among spiking methods and among soils. This supports previous studies that found that speciation of metals in soils depends on soil properties, metal concentrations, and source of metal addition (Manceau et al., 2002; Jacquat et al., 2009a; Walraven et al., 2015). Also, the results demonstrated that the commonly used nitrate spiking method produced significantly lower Zn and Ni concentrations, but had little effect on Pb concentrations. This indicates that the metal salt spiking method is the most susceptible to soil properties, especially pH. The low pHs of the soils used in this study enhanced the transport of metal ions from the soils. Suppose the pHs of the soils were neutral or alkaline, Zn^{2+} ions would have formed surface complexes with secondary minerals, precipitates with carbonate, phosphate, hydroxide, and sulphate. Consequently, the amount of metal ions leached out of the soils would be much less. For purposes of studying how toxic metals are to plants or other organisms, the metal salt spiking method presents other challenges aside low metal concentrations: regarding metal mixture experiments, which require a constant ratio of metals, leaching with artificial rain water will ruin the fixed ratio of metals in soils. In addition, aqueous base cations present in the soils are likely to be leached out, resulting in a change in soil chemical properties. In clay soils, an attempt to leach out salts may create water logged conditions, which in turn will lead to a decrease in dissolved oxygen content and eventually anaerobic conditions. The ultimate impact will be the decrease in microbial population and diversity.

Generally, the oxide spiking method yielded metal concentrations higher than the target concentrations; it is not clear why this was the case. Probably, errors in metal oxide measurements led to the increase in metal concentrations. Aside ZnO and background Zn species, the presence of other Zn species in the oxide spiked soils was due to the partial dissolution of ZnO particles, which was caused by the acidic nature of the soils. If the pH of the soils were ≥ 7, ZnO oxide would have been the only species present because ZnO particles are sparingly soluble under neutral and alkaline soil conditions. As a result, with regards to soil toxicity studies, the oxide spiking method may not be appropriate for soils with pH ≥ 7. Contrary to the nitrate spiking method, the oxide spiking method does not create any artifacts in the soil, except an increase in pH in the immediate surrounding of the dissolving ZnO particles (Voegelin et al., 2011).

In most cases, the annealed spiking method replicated the target concentrations of Zn, Pb and Ni; however, franklinite and outer-sphere/aqueous Zn were the only Zn species found in the annealed spiked soils. The latter's presence is probably due to the slight dissolution of the former. Toxicity studies usually involve the exposure of organisms to mostly free metal ions; the insolubility of franklinite and other primary metal bearing minerals implies that they are not appropriate for studying how harmful metals are to organisms. If they are to be used, the soils must be acidic, and a long residence time is required to allow the gradual dissolution of the minerals. The second condition may prove to be time consuming. However, concerning risk assessment and the design of remediation techniques for metal contaminated sites, the presence franklinite and other insoluble metal bearing minerals are important, especially to the cost of soil remediation.

3.6 Conclusion

This study set out to determine the spiking method that is more appropriate for soil toxicity and risk assessment studies. It has been demonstrated that the commonly used metal salt method has several drawbacks and hence it is not recommended for use in soil toxicity and risk assessment studies. The two alternative spiking methods (annealed metal and metal oxide) can be used; however, the soil chemical properties, especially soil pH, must be taken into account when these methods are employed. The current study was limited to the individual evaluation of these three spiking methods.

Since the results showed that the individual methods produced only a fraction of all Zn species present in smelter-affected soils, it is therefore suggested that to develop a standard method of metal addition to soils, a study which focuses on a combination of spiking methods is required. Drawing from previous studies that characterized the speciation of metals in smelter-affected soils, the proposed research can develop a method that mimics the fraction and concentration of metal species in smelter-affected soils.

4 Effects of Chemical Speciation on the Bioaccessibility of Zinc and Lead in Spiked and Smelter-Affected Soils

4.1 Preface

The Zn K-edge spectra and LCF results from the spiked soils in Chapter 3 revealed that Zn speciation differed among the soils as a result of variation in soil properties and method of metal addition. In this chapter, *in vitro* tests were complemented with synchrotron based Zn speciation studies of the residual pellets to determine the species of Zn that are likely to contribute to Zn bioaccessibility in the human stomach and duodenum. Speciation of Pb in the spiked soils, and the Pb species that may contribute to Pb bioaccessible concentration were inferred from XRD analysis and the Zn speciation results.

This chapter is in preparation for publication in the Journal of Environmental Quality. The following people assisted with parts of the work carried out in this chapter:

Brian Laird – *In vitro* bioaccessibility test
Katherine Stewart – Statistical analysis of bioaccessibility results
Jordan Hamilton – Collection and analysis of Zn K-edge XANES spectra

4.2 Abstract

Prior studies have suggested that risk assessment of metal contaminated soils should be based on the speciation of metals in soils rather than the total metal content. It has been hypothesized that soil properties and indirect processes transform metal elements into different species; with respect to dissolution, these metal species behave differently under changing soil pH. Consequently, under gastrointestinal conditions, metal species will contribute differently towards metal bioaccessibility.

To test this hypothesis, a combination of synchrotron based X-ray diffraction (XRD), X-ray absorption near edge structure (XANES) and linear combination fitting (LCF) were used to identify the Zn speciation in spiked and smelter-affected soils, and the species of Pb in spiked soils. After conducting *in vitro* digestion tests on these soil samples, XANES and LCF analyses were carried out on the residual pellets to identify the species of Zn and Pb that remained after digesting the soils in pH 1.4 and 6.3 gastric and duodenal fluids, respectively. The metal species that were not present in the residual pellets were shown to contribute the most ions towards metal bioaccessibility. It was demonstrated that ZnO, sphalerite (ZnS), and outer-sphere/aqueous Zn contribute more to Zn bioaccessibility than franklinite ($ZnFe_2O_4$) and Zn incorporated into a hydroxy interlayer mineral (Zn-HIM). Residence time was found to affect the dissolution of Zn-Al LDH; its resistance to dissolution increased with residence time. Hydrocerussite [$Pb_3(CO_3)_2(OH)_2$] and PbO readily released Pb^{2+} into the digestive fluids, leading to high bioaccessible Pb concentrations. It was also observed that, compared to the stomach, the relatively high pH of the duodenum may allow the formation of metal precipitates and organo-metal complexes leading to a reduction in bioaccessible metal concentration.

4.3 Introduction

The potential harmful effects of metals are well documented; this has prompted governments and stakeholders to establish measures to minimize the risks associated with these metals. For contaminated soils, exposure to metals are reduced by meeting remediation goals, which are established after an estimation of the nature and probability of adverse health effects in humans and organisms that may be exposed to the contaminated soils (USEPA, 2007). Incidental ingestion of contaminated soils is a major route through which organisms become exposed to metals. Hence, when estimating the risk of metal contaminated soils, risk assessment usually incorporates oral bioaccessibility, which is the fraction of a metal that is released into the GIT and is available for absorption (Ruby et al., 1999). Oral bioaccessibility is measured from *in vitro* tests as the ratio of the mass of a metal dissolved into a volume of simulated digestive fluid to the mass of the metal in the soil sample (Kelley et al., 2002). It is a fast and inexpensive method for estimating human exposure to metals and serves as a surrogate for oral bioavailability, which is defined by the USEPA as ”the fraction of an ingested dose that crosses the gastrointestinal epithelium and becomes available for distribution to internal target tissues and organs” (USEPA, 2007). Furthermore, results from oral bioaccessibility tests could be crucial to the development and assessment of remedial techniques such as soil washing and soil amendments (Ruby et al., 1999).

Currently, Canadaian regulations and environmental guidelines are predicated on the assumption that the total amount of a metal in a contaminated soil is bioaccessible (Koch et al., 2013). Although total metal concentration is indicative of the degree of contamination, studies have shown that it has little relationship with bioaccessibility (Sparks, 2003). Hence this approach could lead to the overestimation of the risks posed by metal contaminated soils. This is because the desorption of metals from soil particles into any aqueous medium surrounding it (e.g soil water and gastric fluid) is controlled by soil properties including soil texture, pH, CEC, redox conditions, organic matter content, the presence of anionic species (such as carbonates, phosphates, chloride, sulfides hydroxides and organic acids) that form complexes with metal cations, and the duration of contact between the metal and soil (Richardson et al., 2006). These factors either inhibit or promote the solubility of metals in soils by influencing their speciation. It thus follows that bioaccessibility of a soil contaminated with metals is largely

dependent on the chemical speciation of the metals. Taking this into account will ensure a more accurate estimation of the potential exposure and related risks presented by metal contaminated soils. Although many studies have made strong connections between chemical speciation and bioaccessibility, not much research has been done to establish the effects of the former on the latter. Consequently, this chapter aimed to identify the species of Zn and Pb in spiked and smelter-affected soils that contribute metal ions into simulated gastric and duodenal fluids. It was hypothesized that Zn and Pb bearing primary minerals, and Zn and Pb specifically adsorbed to soil mineral surfaces will contribute less metal ions into digestive fluids than secondary minerals and non-specifically adsorbed species.

4.4 Materials and Methods

4.4.1 Soil samples and treatments

Twenty seven spiked soil samples from the previous chapter plus two soils from a smelter-affected area in Flin Flon, MB were used in this study. The smelter-affected soils were selected from seven soil samples studied by Hamilton et al. (2016a). The seven soils were sampled at surface (0-2 cm) and subsurface (8-10 cm); they were separated by distance and direction from the smelter, slope position, vegetative cover, and chemical properties. In general, the soils belonged two groups. The first group occurred at the upper slope position with minimal vegetation, and was prone to wind and water erosion; the second group occurred at more stable areas at the bottom slope positions, and was colonized by metal tolerant grass (Hamilton et al., 2016a). Based on these differences, one soil, taken at a depth of 8-10 cm, was selected from each group; they are labeled eroding and stabilized from group one and two, respectively. The 29 soil samples used for this study were ground using mortar and pestle. Total concentrations of Zn and Pb in these soils were determined using XRF; results are provided in Table 4.1. The bioaccessible concentrations of Zn and Pb in each of the 29 soils were determined using a modified physiological based extraction test (PBET) (Laird et al., 2015). The gastric and duodenal phases each consisted of 29 treatments for a total of 58 treatments, repeated in triplicate for a total of 174 experimental units.

Table 4.1: Total Zn and Pb concentrations in the 27 spiked soils used for the bioaccessibility measurements.

	3.22 Soil		WTRS Soil		UBC Soil	
	Zn	Pb	Zn	Pb	Zn	Pb
	$\mu g\, g^{-1}$					
FF[†] -Ox[‡]	7770	1130	6680	276	5870	68
FF-Anl[§]	5810	1230	4420	468	3800	409
FF-Nit[¶]	1690	1330	1280	628	846	460
PC[#]-Ox	2210	864	1860	348	552	110
PC-Anl	1620	775	1610	222	316	99
PC-Nit	1380	856	1170	267	183	135
SB[††]-Ox	4890	5290	3830	2780	2780	3920
SB-Anl	4460	6440	2680	5240	3800	6780
SB-Nit	1800	5740	1510	5820	339	4670

[†] Flin Flon mixture
[‡] Oxide spiking method
[§] Annealed spiking method
[¶] Nitrate spiking method
[#] Port Colborne Mixture
[††] Sudbury mixture

4.4.2 *In vitro* gastric model

Gastric fluid, which was basically pH 1.4 doubly deionized H_2O, was prepared by dropwise addition of 12 M HCl. 40 mL of the solution was transferred into acid-washed penicillin bottles containing 0.4 g of soil. The pH of the slurry was determined to ensure it was between 1.4 and 1.6. Those that were below and above the range were adjusted by dropwise addition of 0.5 M NaOH or 0.5 M HCl, respectively. The bottles were then capped and put in an incubator shaker set at 130 rpm and 37 °C for 2 hours. After 40 and 80 minutes of shaking, 10 mL aliquots of the slurry were pipetted into 15 mL falcon tubes and centrifuged at 5000g for 10 minutes. After 120 minutes of shaking, the 20 mL slurry left was transferred into 50 mL Falcon tubes and centrifuged at 5000g for 10 minutes. The supernatant was then transferred into 15 mL Falcon tubes for chemical analysis. The residual pellets were dried in a fume hood for XANES analysis.

4.4.3 *In vitro* duodenal model

Forty mL of gastric solution was transferred into acid-washed penicillin bottles containing 0.4 g of soil. The pH of the slurry was adjusted to between 1.4-1.6 by dropwise addition of 0.5 M NaOH and 0.5 M HCl, respectively. The bottles were then capped and put in an incubator shaker set at 130 rpm and 37 °C for 2 hours. After 2 hours, the bottles were uncapped and 20 mL of duodenal solution (12.5 g L^{-1} $NaHCO_3$, 6 Oxgall g L^{-1} and 0.9 g Pancreatin) was added. The pH of the new solution was determined to ensure it was between 6.3-6.7; adjusted by dropwise addition of 0.5 M NaOH or 0.5 M HCl, when necessary. The bottles were then capped and put in an incubator shaker set at 130 rpm and 37 °C for another 2 hours. After 160 and 200 minutes of shaking, 10 mL aliquots of the slurry were pipetted into 15 mL Falcon tubes and centrifuged at 5000g for 10 minutes. The 20 mL slurry left after 240 minutes of shaking was transferred into 50 mL Falcon tubes and centrifuged at 5000g for 10 minutes. The supernatants were then transferred into 15 mL falcon tubes and 3% HCl solution was added to preserve them for chemical analysis. The residual pellets were dried in the fume hood for XANES analysis.

4.4.4 Chemical analysis

The concentrations of Zn and Pb released into the simulated fluids were determined using an Agilant 4100 Microwave Plasma Atomic Emission Spectrometer (MP-AES). For each batch of extraction, a standard reference material (NIST 2711 Montana Soil) was included for quality control. Recovery percentages for the eight batches ranged from 26.17-28.29% Zn and 88.84-92.95% Pb in the stomach; 6.12-8.35% Zn and 2.53-2.83% Pb in the duodenum. Also, two blanks were included in each batch of extraction, and in cases where Zn and Pb concentrations exceeded the instrumental limit of detection, the average of the blank concentrations were subtracted from the sample concentrations.

4.4.5 Statistical Analysis

Bioaccessibility is usually reported as the ratio of mass of metal released into simulated fluids to the mass of metal in soil. However, due to the sampling of soil slurry at different time points during the *in vitro* digestion tests, it was difficult to determine

the mass of soil present at 80 and 120 minutes (gastric digestion), and 200 and 240 minutes (duodenal digestion). As a result, the fraction of Zn and Pb released into the simulated fluids could not be calculated. The inability to calculate the percent bioaccessibility lead to the analysis of bioaccessible Zn and Pb concentrations.

A linear mixed-effects (LME) analysis was performed in R (v 3.3.3 Another Canoe) (R Core Team, 2017) using the lme4 package (Bates et al., 2015) . To determine whether bioaccessible Zn and Pb concentrations were affected by the parameters (soil, spiking method and mixture), and whether bioaccessible concentrations differed with time within each treatment, two models [bioacessibility $\sim$ soil+spiking method+mixture+time + (1|treatment)] and [bioacessibility $\sim$ soil*spiking method* mixture*time + (1|treatment)] were compared using the likelihood ratio test. Since three responses were taken from each treatment, the issue of non-independence was resolved by specifying random intercepts for each treatment (1|treatment). Soil, spiking method, mixture ratio, and time were fixed factors. All data were log transformed prior to each analysis and diagnostic plots (fitted vs residual, and qqplot) were used to test model assumptions. In the case of duodenal bioaccessible Zn, time was not included in the analysis because its inclusion violated model assumptions and produced a poor model fit. The likelihood ratio test showed that the model with interactions [bioacessibility $\sim$ soil*spiking method*mixture*time + (1|treatment)] significantly ($\chi^2(54) = 382.31, p < 2.2 \times 10^{-16}$) explained the data. Afterwards, an Anova test (Satterthwaite approximation for degrees of freedom) ($\alpha = 0.05$) was performed to determine the confidence in the estimate of the effects of the fixed factors on Zn and Pb bioaccessibility. Finally, a Tukey's HSD ($\alpha = 0.05$) was used to compare the mean bioaccessible Zn and Pb concentrations. Anova tables are provided in the appendix.

4.4.6 X-ray absorption spectroscopy (XAS) analysis

X-ray absorption near edge structure (XANES) analysis was performed on the two smelter-affected soils, their residual pellets, and the residual pellets from the spiked samples (Flin Flon mixture). Zn K-edge (9659 eV) spectra of these samples were collected at the Hard X-ray Microanalysis (HXMA) beamline at the CLS. The CLS storage ring operated at 2.9 GeV and the beam current varied between 150-250 mA. The beamline monochromator consisted of a Si-220 crystal adjusted to a spot size of 0.5-

1.5×0.7-2.5 mm. The monochromator was detuned by 50% to reduce higher harmonics and calibrated to the first inflection point of the K-edge Zn reference foil of 9659 eV. The XANES spectra for all samples were collected in fluorescence mode at ambient temperature with a 32-element Ge detector (Canberra); a Cu-6 filter and Soller slits were placed between the sample and detector to reduce scattering and unwanted fluorescence from other elements. Aluminum foil was also placed over the 32-element detector to improve signal to noise by preferentially reducing Fe fluorescence from samples. For each sample, 2-3 scans were collected, depending on metal concentration. All XANES spectra were analyzed with ATHENA (Ravel & Newville, 2005). Briefly, the background was subtracted and calibrated to the Zn reference foil (9659 eV). Scans were smoothed when necessary and the absorption edge was set at the zero crossing of the second derivative. Individual scans of each sample were then merged. Using a spectral library of Zn standard compounds prepared by (Hamilton et al., 2016a), the semi-quantitative approach of linear combination fitting was used to retrieve the contribution of each standard spectrum to each sample spectrum. The fitting range for XANES data was between 9640-9740 eV.

4.5 Results

4.5.1 Zn and Pb bioaccessibility

The LME analysis showed that mean gastric and duodenal bioaccessible Zn concentrations significantly differed ($p < 0.001$) between soils, spiking methods and mixture; the interactions between these factors was also significant ($p < 0.001$). The effect of time was almost the same between the three time points ($p = 0.98$). The effect of time on mean gastric bioaccessible Zn concentrations was significantly different ($p < 0.001$) between treatments; however, the effect of time on bioaccessible concentration between treatments was not an objective in this study. For gastric bioaccessible Pb concentrations, the effect of soils, mixture, and spiking method were significant ($p < 0.001$). Except for spiking method ($p = 0.05$), soil and mixrture had significant effects ($p < 0.001$) on duodenal bioaccessible Pb concentrations. Since bioaccessibile Zn and Pb concentrations did not vary between time points, only bioaccessible concentrations at 120 and 240 minutes (gastric and duodenum, respectively) are presented.

The bioaccessible Zn concentrations, grouped according to mixture, spiking method, and soil, are shown in Fig. 4.1. Bioaccessible Zn concentrations decreased from the gastric phase (pH 1.4) to the duodenal phase (pH 6.3); this is consistent with previous studies that found that metal boaccessibility decreased with increase in pH (Oomen et al., 2002). A comparison of bioaccessible concentrations for the three spiking methods indicated that bioaccessible Zn concentration was sensitive to the method of metal addition. In both gastric and duodenal phases, the oxide spiked soils yielded significantly higher ($p<0.05$) bioaccessible Zn concentrations than the annealed and nitrate spiked soils (Fig. 4.1). Except for the Flin Flon mixture, where the annealed spiked soils had significantly higher bioaccessible Zn concentrations than the nitrate spiked soils, there was no clear difference between the annealed and nitrate spiked soils for the Port Colborne and Sudbury mixtures. Generally, the Flin Flon mixture, which contained the highest total Zn concentration (Table 4.1), produced the highest Zn bioaccessible concentrations. Although bioaccessible Zn concentrations differed between soils, no clear pattern was observed (Fig. 4.1).

Similarly, bioaccessible Pb concentrations decreased from the gastric to the duodenal phase. In contrary to Zn, spiking method had little and no effect on gastric and duodenal bioaccessible Pb concentrations, respectively; differences were observed in the gastric phase, but no specific trend emerged (Fig. 4.2). The same can be said about differences in bioaccessible Pb concentrations between the three soils (Fig. 4.2). The only factor that greatly affected bioaccessible Pb concentrations was mixture. The Sudbury mixture, which had the highest Pb concentration, yielded significantly higher ($p<0.05$) values in both gastric and duodenal phases. Generally, compared to the Port Colborne mixture, the Flin Flon mixture had significantly higher bioaccessible Zn concentrations (Fig. 4.2). For the smelter-affected soils, the stabilized soil yielded higher bioaccessible Zn concentrations than the eroding soil; in the stabilized soil 9.2 ± 0.02 μg Zn mL^{-1} and 4.4 ± 0.2 μg Zn mL^{-1} were recorded for the gastric and duodenal phases, respectively. The eroding soil yielded 1.8 ± 0.04 μg Zn mL^{-1} and 0.8 ± 0.02 μg Zn mL^{-1} in the stomach and duodenum, respectively.

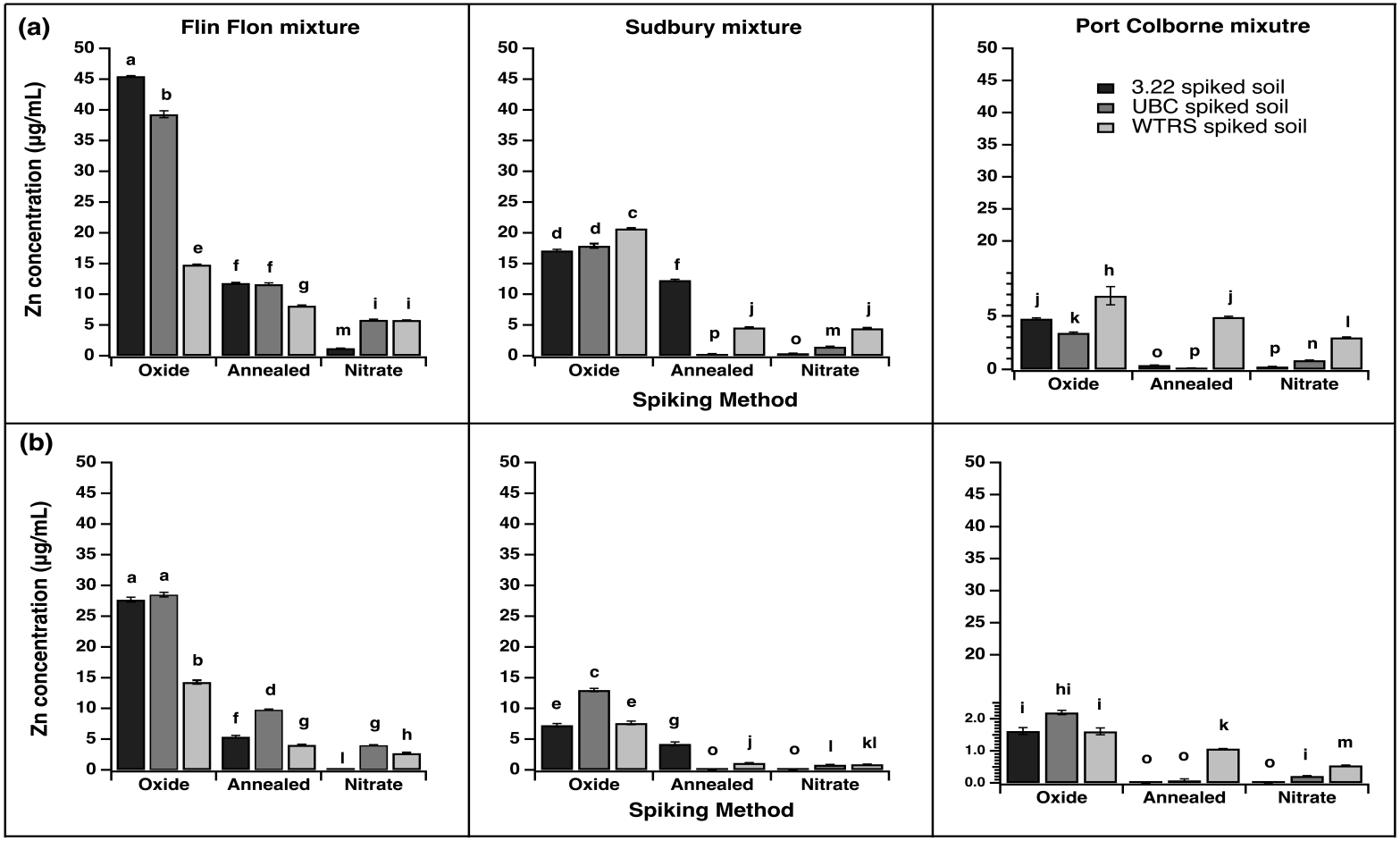

Fig. 4.1: Bioaccessible Zn concentrations compared across 3 factors: mixture (Flin Flon, Sudbury and Port Colborne), spiking method (oxide, annealed, and nitrate) and soil (3.22, UBC, and WTRS). Since time was not a significant predictor of bioaceessibility, only bioaccessible concentrations after 120 and 240 minutes are presented in this graph for stomach and duodenum, respectively. (a) represents stomach and (b) duodenum. Bars with the same lowercase alphabets are not significantly different.

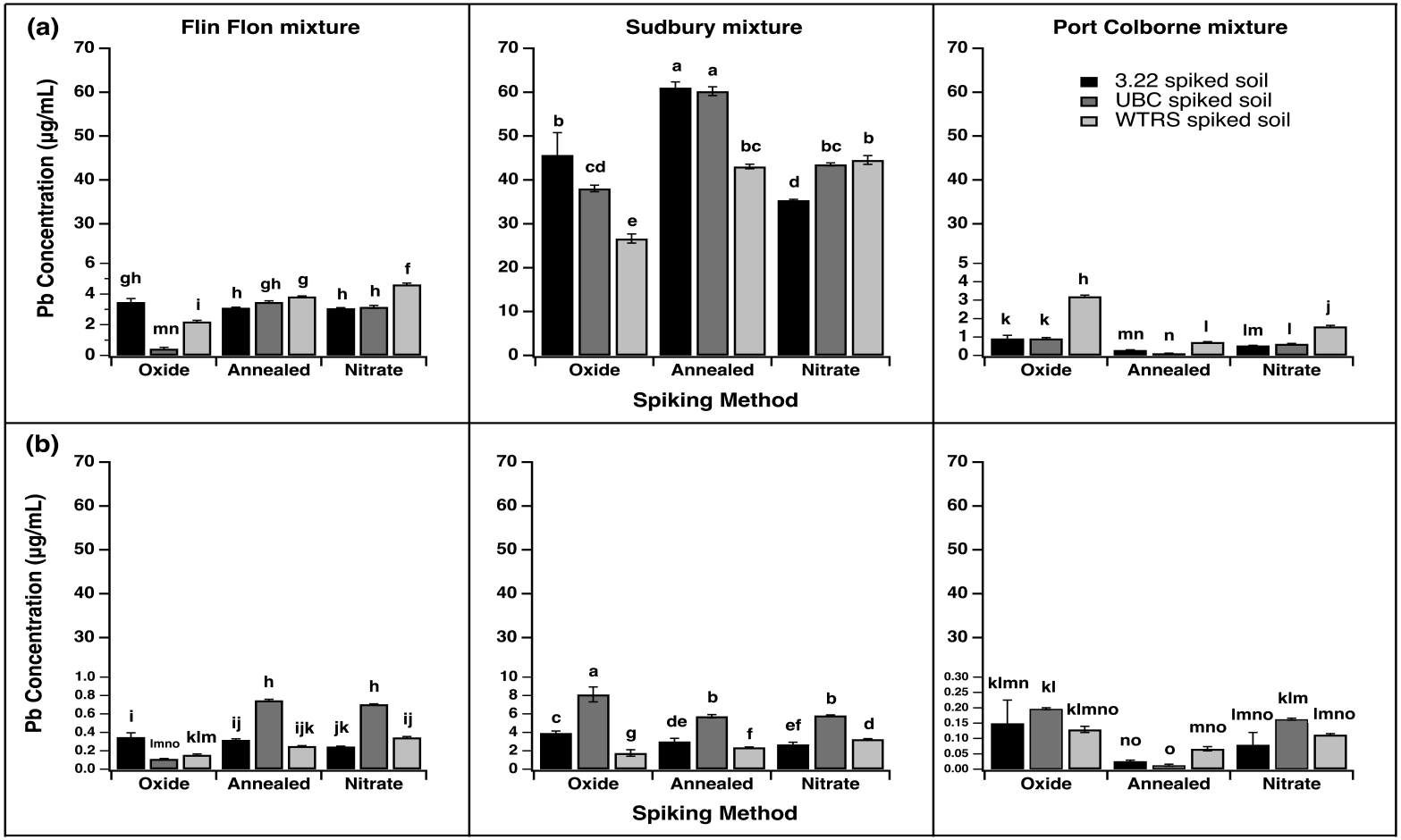

Fig. 4.2: Bioaccessible Pb concentrations compared across 3 factors: mixture (Flin Flon, Sudbury and Port Colborne), spiking method (oxide, annealed, and nitrate) and soil (3.22, UBC, and WTRS). Since time was not a significant predictor of bioaceessibility, only bioaccessible concentrations after 120 and 240 minutes are presented in this graph for stomach and duodenum, respectively. (a) represents stomach and (b) duodenum. Bars with the same lowercase alphabets are not significantly different.

4.5.2 Zn speciation in residual pellets

To determine the species of Zn that contributed to its bioaccessible concentration in the stomach and duodenum, Zn K-edge XANES spectra were collected from the dried residual pellets after the *in vitro* gastric and duodenal soil digestions. The Zn K-edge spectra and corresponding LCF models for spiked and smelter-affected soils, and their residual pellets are shown in Fig. 4.3. The XANES spectra from the smelter-affected soils were markedly different, suggesting that the species of Zn in these two soils were different. For the eroding soil, the LCF analysis showed that total Zn comprised 68% franklinite, 11% sphalerite, and 18% outer-sphere/aqueous Zn (Table 4.2). The total Zn in the stabilized soil consisted of 17% frankinite, 21% Zn-HIM, 28% Zn-Al LDH, and 32% outer-sphere/aqueous Zn (Table 4.2). It was found in the previous chapter that franklinite, sphalerite, and aqueous Zn were present in all 3.22 spiked soils at varying relative abundance; ZnO was the only species unique to the oxide spiked 3.22 soil. However, all the spectra from the 3.22 residual pellets (both gastric and duodenum) were adequately reproduced without sphalerite and ZnO (Table 4.3). This suggests that sphalerite and ZnO completely dissolved in the simulated stomach and duodenum. The complete disappearance of ZnO was also observed in the residual pellets from the WTRS and UBC spiked soils (Tables 4.4 and 4.5). In the eroding soil, however, the LCF analysis showed that the fraction of sphalerite decreased from 12% to 5% in the simulated stomach, indicating that a small fraction of sphalerite remained after the 2 hr gastric digestion (Table 4.2). For the same soil, no trace of sphalerite was found in the duodenal residual pellet (Table 4.5). Franklinite, on the other hand, persisted in both the stomach and duodenum. However, except for the stabilized soil, its fraction increased after the gastric digestion, and decreased after the duodenal digestion (Table 4.2). This same trend was observed in the residual pellets from the annealed spiked 3.22, WTRS and UBC residual pellets (Tables 4.3, 4.4 and 4.5). In the annealed spiked WTRS residual pellets, the fraction of Zn adsorbed on goethite decreased by 2% in the stomach, but increased by 30% in the duodenum. For the nitrate spiked WTRS soil, no trace of Zn adsorbed on goethite was found in the residual pellets after both simulated gastric an duodenal extractions. A similar speciation shift was observed in the oxide spiked WTRS soil after the gastric digestion; however, in the duodenum, Zn adsorbed on goethite decreased by only 4% (Table 4.3). Zn-Al LDH formed 35% of the total Zn fraction in the oxide spiked WTRS soil, but after the simulated gastric and

duodenal soil digestions, it formed no part of Zn species in the gastric and duodenal residual pellets (Table 4.3). In contrast, the fraction of Zn-Al LDH in the stablized soil remained almost the same after both the gastric and duodenal digestions (Table 4.2). The stabilized and nitrate spiked UBC soils contained 21 and 24% Zn-HIM, respectively. After the digestion experiments, the gastric and duodenal residual pellets from the stabilized soil were found to contain 21 and 22% Zn-HIM respectively (Table 4.2). In the gastric residual pellet from the nitrate spiked UBC sample, no Zn-HIM was found, but it accounted for 18% of the total Zn in the duodenal residual pellet (Table 4.5). The LCF results for the nitrate and oxide spiked WTRS soils showed that Zn-HIM was not present in these soils; however, after the *in vitro* digestions, Zn-HIM was detected in both gastric and duodenal residual pellets (Table 4.4). It was expected that outer-sphere Zn would be easily displaced into the simulated fluids during digestion; this was the case with the annealed spiked 3.22, WTRS, and UBC soils that contained 23, 26, and 21% outer-sphere Zn, respectively (Tables 4.3, 4.4, and 4.5). Furthermore, in both the eroding and stabilized soils, which contained 18 and 32% outer-sphere Zn, respectively, the LCF analysis showed that outer-sphere Zn was not present in any of the residual pellets (Table 4.2). However, for the oxide spiked 3.22 soil and the nitrate spiked UBC samples, outer-sphere Zn was still present in the residual pellets (Tables 4.3 and 4.5).

Except for the oxide spiked UBC soil, which contained $ZnCO_3$, none of the soil samples contained $ZnCl_2$ and/or $ZnCO_3$ prior to the digestion experiments (Tables 4.2, 4.3, 4.4, and 4.5). However, none of the XANES spectra from the gastric residual pellets was adequately modeled without $ZnCl_2$, and none of the XANES spectra from the duodenal residual pellets was adequately reproduced without $ZnCl_2$ and $ZnCO_3$, except for the residual pellet from the oxide spiked WTRS soil (Tables 4.2, 4.3, 4.4, and 4.5). These results indicate that the Zn^{2+} ions released from the dissolution of soluble Zn species reacted with ligands (Cl^- and ${CO_3}^{2-}$) to form secondary species.

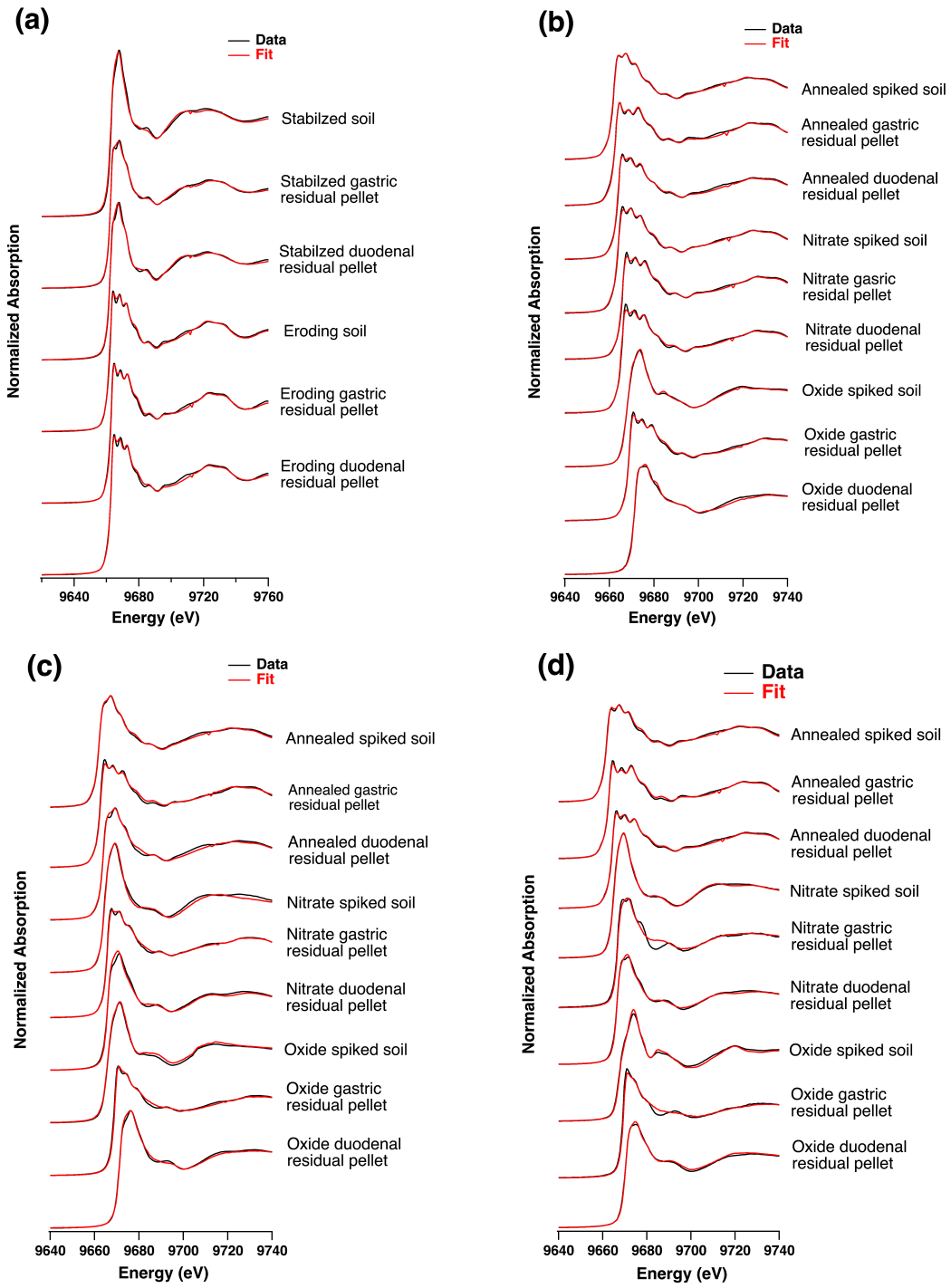

Fig. 4.3: Zn K-edge XANES spectra (black lines) and linear combination fits (red lines) for (a) smelter-affected soils (stabilized and eroding) from Flin Flon, MB, and their respective gastric and duodenal residual pellets; (b), (c) and (d) represent 3.22, WTRS and UBC spiked (annealed, nitrate and oxide) soils, respectively and their corresponding gastric and duodenal residual pellets. LCF results are provided in Tables 4.2, 4.3, 4.4 and 4.5 for (a), (b), (c), and (d), respectively.

Table 4.2: Total and bioaccessible Zn concentrations and XANES Linear Combination fits (LCF) results for the smelter-affected soils (stabilized and eroding) and residual pellets.

	Total[†]	Bioaccessible								
ID	Zn	Zn	Franklinte ($ZnFe_2O_3$)	Sphalerite (ZnS)	Zn-HIM[‡]	Zn-Al LDH[§]	$ZnCO_3$	$ZnCl_2$	Outer-sphere/ $Zn^{2+}_{(aq)}$	Reduced χ^2
	- - μg g^{-1} - -	- - μg mL^{-1} - -	- % -							
Eroding	3170	-	68	11	-	-	-	-	18	2.4×10^{-4}
Eroding Gastric[¶]	3170	1.81 ± 0.04	70	5	-	-	-	26	-	2.3×10^{-4}
Eroding Duodenum[#]	3170	0.82 ± 0.02	60	-	-	-	19	19	-	2.9×10^{-4}
Stabilized	4580	-	17	-	21	28	-	-	32	6.3×10^{-4}
Stabilized Gastric[¶]	4580	9.42 ± 0.12	22	-	21	25	-	30	-	1.3×10^{-4}
Stabilized Duodenum[#]	4580	4.39 ± 0.16	29	-	22	29	28	-	-	2.6×10^{-4}

[†] Total Zn concentration measured with X-ray fluorescence
[‡] Zinc hydroxy interlayered mineral
[§] Zn aluminum layered double hydroxide
[¶] Residual pellet from gastric digestion
[#] Residual pellet from duodenal digestion

Table 4.3: Total and bioaccessible Zn concentrations and XANES Linear Combination fits (LCF) results for 3.22 spiked soil and residual pellets.

	Total[†]	Bioaccessible							
ID	Zn	Zn	Franklinte ($ZnFe_2O_3$)	Sphalerite (ZnS)	ZnO	$ZnCO_3$	$ZnCl_2$	Outer-sphere/ $Zn^{2+}_{(aq)}$	Reduced χ^2
	- - $\mu g\ g^{-1}$ - -	- - $\mu g\ mL^{-1}$ - -	- % -						
Annealed	5810	-	66.5	6.4	-	-	-	24.8	6.5×10^{-5}
Annealed Gastric[‡]	5810	11.83 ± 0.12	80	-	-	-	18	-	1.4×10^{-4}
Annealed Duodenum [§]	5810	5.40 ± 0.21	56	-	-	19	23	-	1.7×10^{-4}
Nitrate	1690	-	74	4	-	-	-	20	1.6×10^{-4}
Nitrate Gastric[‡]	1690	1.2 ± 0.01	75	-	-	-	11	12	2.0×10^{-4}
Nitrate Duodenum[§]	1690	0.11 ± 0.00	63	-	-	20	15	-	3.2×10^{-4}
Oxide	7770	-	23	11	28	-	-	39	1.1×10^{-4}
Oxide Gastric[‡]	7770	45.53 ± 0.09	59	-	-	-	32	28	7.2×10^{-4}
Oxide Duodenum[§]	7770	27.68 ± 0.40	21	-	-	-	42	34	2.3×10^{-4}

[†] Total Zn concentration measured with X-ray fluorescence
[‡] Residual pellet from gastric digestion
[§] Residual pellet from duodenal digestion

Table 4.4: Total and bioaccessible Zn concentrations and XANES Linear Combination fits (LCF) results for WTRS spiked soil and residual pellets.

ID	Total[†] Zn	Bioaccessible Zn	Franklinte ($ZnFe_2O_3$)	Zn-Al LDH[‡]	Zn-HIM[§]	ZnO	$ZnCO_3$	$ZnCl_2$	Zn-Sorbed Goethite	Zn-Sorbed Outer-sphere/ $Zn^{2+}_{(aq)}$	Reduced χ^2
	- - $\mu g\ g^{-1}$ - -	- - $\mu g\ mL^{-1}$ - -	- % -								
Annealed	4420	-	54.8	-	-	-	-	-	16	26	1.4×10^{-4}
Annealed Gastric[¶]	4420	8.15 ± 0.05	60	-	-	-	-	25	14	-	4.5×10^{-4}
Annealed Duodenum[#]	4420	4.07 ± 0.06	38	-	-	-	-	13	47	-	4.5×10^{-4}
Nitrate	1280	-	-	-	-	-	-	-	96	-	3.7×10^{-4}
Nitrate Gastric[¶]	1280	5.83 ± 0.06	34	-	20	-	-	44	-	-	2.3×10^{-4}
Nitrate Duodenum[#]	1280	2.74 ± 0.11	-	-	30	-	30	28	-	-	6.3×10^{-4}
Oxide	6680	-	-	35	-	16	-	-	49	-	1.1×10^{-4}
Oxide Gastric[¶]	6680	14.83 ± 0.10	19	-	7	-	-	73	-	-	6.0×10^{-4}
Oxide Duodenum[#]	6680	14.29 ± 0.29	15	-	12	-	-	27	46	-	3.0×10^{-4}

[†] Total Zn concentration measured with X-ray fluorescence
[‡] Zn aluminum layered double hydroxide
[§] Zinc hydroxy interlayered mineral
[¶] Residual pellet from gastric digestion
[#] Residual pellet from duodenal digestion

Table 4.5: Total and bioaccessible Zn concentrations and XANES Linear Combination fits (LCF) results for UBC spiked soil and residual pellets.

	Total[†]	Bioaccessible								
ID	Zn	Zn	Franklinte ($ZnFe_2O_3$)	Zn-HIM[‡]	ZnO	ZnC_2O_4	$ZnCO_3$	$ZnCl_2$	Outer-sphere/ $Zn^{2+}_{(aq)}$	Reduced χ^2
	-- $\mu g\ g^{-1}$ --	-- $\mu g\ mL^{-1}$ --	---------- % ----------							
Annealed	3800	-	76.9	-	-	-	-	-	21	2×10^{-5}
Annealed Gastric[§]	3800	11.65 ± 0.21	85	-	-	-	-	14	-	2.2×10^{-4}
Annealed Duodenum[¶]	3800	9.76 ± 0.11	62	-	-	-	17	18	-	1.5×10^{-4}
Nitrate	846	-	-	24	-	-	46	-	28	1.2×10^{-4}
Nitrate Gastric[§]	846	5.85 ± 0.11	-	-	-	-	36	51	13	2.0×10^{-4}
Nitrate Duodenum[¶]	846	4.01 ± 0.09	-	18	-	-	-	38	42	2.4×10^{-4}
Oxide	5870	-	-	-	53	-	43	-	-	5.0×10^{-4}
Oxide Gastric[§]	5870	39.29 ± 0.55	-	6	-	-	-	93	-	1.2×10^{-4}
Oxide Duodenum[¶]	5870	28.52 ± 0.36	-	-	-	26	43	31	-	2.4×10^{-4}

[†] Total Zn concentration measured with X-ray fluorescence
[‡] Zinc hydroxy interlayered mineral
[§] Residual pellet from gastric digestion
[¶] Residual pellet from duodenal digestion

4.6 Discussion

4.6.1 Metal species that contribute to bioaccessible concentrations

The objective of this study was to determine the species of Zn and Pb in contaminated soils that contribute to their bioaccessible concentrations in *in vitro* gastrointestinal models. It was hypothesized that Zn and Pb bearing primary minerals, and Zn and Pb specifically adsorbed to soil mineral surfaces will contribute less metal ions into digestive fluids than secondary minerals and non-specifically adsorbed species. The Zn K-edge spectra from the soils and residual pellets along with the LCF results, to a large extent, support this hypothesis, and also corroborate previous studies that have suggested that metal bioaccessibility is mainly dependent on chemical speciation.

It was observed that Zn species that are readily soluble under acidic soil conditions behave in a similar manner under stomach conditions. The Zn^{2+} ions released into the simulated gastric and duodenal fluids was partly due to the complete dissolution of ZnO, sphalerite and the displacement of outer-sphere Zn from the surfaces of soil particles. The dissolution of ZnO is consistent with previous studies that showed that ZnO is a readily soluble source of Zn in low pH soils (Voegelin et al., 2005; Voegelin et al., 2011). However, compared to most soils, the pH of the stomach is much lower, and though ZnO dissolution requires two protons (H^+) per Zn, as shown in Eq. 4.1, there are enough protons in the highly acidic stomach to allow the complete dissolution of ZnO. The speciation of Pb in the spiked soils and residual pellets was not investigated in this study; however, it can be inferred from the Zn speciation results that PbO was present in, at least, the oxide spiked soils. Comparable to ZnO, PbO forms under alkaline conditions and it is expected to be unstable under acidic conditions (Ruby et al., 1999; Cao et al., 2008); this explains the high bioaccessible Pb concentrations observed in the oxide spiked soils (Fig. 4.2).

$$ZnO_{(s)} + 2\,H^{+}_{(aq)} \rightleftharpoons Zn^{2+}_{(aq)} + H_2O_{(l)} \qquad \text{(Eq. 4.1)}$$

The rate limiting step for the dissolution of soluble metal oxides, under acidic conditions, is the transport of metal ions from the oxide surface (Sparks, 2003). However, the agitation and mixing of the soil slurry at 130 rpm (mimicking the churning action

in the gut) ensured that metal ions did not accumulate on the oxide surface; this contributed to the complete dissolution of ZnO and PbO within the 2 hr residence time. It can be inferred from Fig. 4.1 and 4.2 that for the mixtures that contained high metal loadings (Flin Flon and Sudbury for Zn and Pb, respectively), the oxide spiked soils, which contained high fractions of Zn and Pb oxides, yielded higher bioaccessible concentrations. This implies that the fraction or concentration of a soluble metal species in soils affects the bioaccessible metal concentration; thus, the higher the soluble metal fraction in the soil, the higher the bioaccessible metal concentration.

In soils and mine tailings, oxidative dissolution is often the mechanism by which sphalerite dissolves, but kinetics studies have found that at pH 1-4, Zn release from sphalerite is initially rapid, followed by a slow dissolution reaction, and the overall rate of dissolution increases with decrease in pH (Weisener et al., 2003; Stanton et al., 2008). Similar results were reported by Acero et al. (2007) also found that at a pH range of 1-4.2, and dissolved O_2 levels of 0.2-8.7 mg L^{-1}, sphalerite dissolution was mediated by H^+ ions, but O_2 concentration did not affect dissolution rate. These findings are in agreement with the observations made in this study. The absence of sphalerite in the stabilized and 3.22 residual pellets clearly shows that sphalerite weathers at low pH. This implies that, if present in incidentally ingested soils, sphalerite will contribute towards the total bioaccessible Zn concentration in the stomach and duodenum. Zn-Al LDH is formed in soils with pH $>$ 5 (Jacquat et al., 2009c); this suggests that lower soil pH does not favor the formation of Zn-Al LDH. Therefore, it may be expected that the stability of Zn-Al LDH will decrease as pH decreases. But results obtained from this study showed that Zn-Al LDH behaved inconsistently under the simulated stomach and duodenum. In the stabilized soil sample, it persisted in both gastric and duodenal fluids (Table 4.2), but in the oxide spiked WTRS soil, the LCF results suggested that it completely dissolved (Table 4.4). Previous studies have reported that the stability of Ni-AL LDH at pH 4 is due to the aging effect on the precipitate (Scheidegger & Sparks, 1996; Scheckel, Scheinost, Ford, & Sparks, 2000; Scheckel & Sparks, 2001). The main mechanism responsible for the stability of Ni-Al LDH with residence time was attributed to the substitution of silica for nitrate within the Ni-Al LDH interlayer, and the subsequent polymerization of silicate in the hydroxide layers (Ford et al., 1999). The aging and silication hypothesis may explain the inconsistent behavior of

Zn-Al LDH observed in the current study; Zn-Al LDH in the field sample certainly aged longer than Zn-Al LDH in the spiked sample (years and 30 days for field and spiked samples, respectively). For outer-sphere Zn species, Zn is held on the surfaces of soil particles by a force of attraction; this weakly bound Zn was expected to be displaced by H^+ ions at low pH. Though this was the case in many of the samples, outer-sphere Zn was found in three residual pellets after the gastric digestion (Tables 4.3 and 4.5). It is probable that after the soil slurry was centrifuged and the chyme decanted, the leftover fluid and pellet still contained aqueous Zn^{2+}. It is also possible that for these samples, not all the electrostactically bound Zn were displaced into the gastric solution.

Some of the Zn species present in the spiked and smelter-affected soils released little to no Zn ions into the simulated fluids. Results from the LCF analysis showed that franklinite was present in the gastric and duodenal pellets (Tables 4.2, 4.3, 4.4 and 4.5) indicating that it sparingly dissolved under the simulated physiological conditions. It has been reported that for franklinite to weather within two hours and release about 90% of the Zn trapped in its matrix, a pH between 0-0.5 and temperature of at least 90 °C are required (Nunez & ViÃśals, 1984). These extreme conditions do not exist in any compartment of the human gut. In addition, franklinite dissolution is likely to be controlled by surface reactions, and the rate limiting step is the detachment of Zn ions from the mineral surface (Sparks, 2003). Thus, the dissolution rate is sensitive to the residence time (2 hrs) in the stomach, which is not long enough to allow franklinite to substantially dissolve. As a result, soils contaminated with predominantly franklinite, if incidentally ingested, will pose little risk. Comparable to franklinite, Zn-HIM is reported to be less soluble even at low soil pH due to the stable bonds between Zn and the hydroxy interlayer-Al polymers in HIM (Jacquat, Voegelin, & Kretzschmar, 2009b). It was therefore expected that Zn-HIM will be sparingly soluble in the simulated stomach and duodenum. Prior to the digestion experiments, the stabilized and nitrate spiked UBC soils were the only samples that contained Zn-HIM (Tables 4.2 and 4.5). The results from the stabilized soil, which suggested that Zn-HIM was insoluble in the simulated stomach and duodenum, are consistent with previous studies. However, the XANES and LCF analysis of the spectra from the nitrate spiked UBC sample showed that Zn-HIM was absent and present in the gastric and duodenal residual pellets, respectively (Table 4.5). The absence of Zn-HIM in the gastric residual pellet suggests

that it dissolved in the 40 mL gastric fluid during digestion; but if this was the case, it should not have been detected in the duodenal residual pellet because the chemical and physical conditions of the gastric phase (pH 1.4, 37 °C, 130 rpm rotational shaking) were exactly the same for the first 2 hr of the duodenal phase. It is possible that the signal of the Zn-HIM in the gastric residual pellet was swamped by the signals from the other Zn species precluding its detection. This explanation may hold for the observations made in the nitrate and oxide spiked WTRS soil samples; Zn-HIM was below detection limits in these soil samples, but was detected in both their gastric and duodenal residual pellets (Table 4.4). The implication of these results is that Zn-HIM is sparingly soluble under highly acidic gastric conditions, and will pose little to no risk to human receptors.

As stated earlier, the speciation of Pb in the spiked soils was not investigated in this study; but the XRD analysis of the synthetic minerals showed that hydrocerussite was the Pb mineral that was produced from the annealing process. It is therefore reasonable to assume that hydrocerussite was present in, at least, the annealed spiked soils. It is also possible that, given its high solubility under acidic soil conditions (JÃÿrgensen & Willems, 1987), hydrocerussite dissolved after it was added to the test soils (pH 3.4-5.6). Either way, in contrary to franklinite, it can be inferred from the high bioaccessible Pb concentrations in the annealed spiked soils (Sudbury mixture) that hydrocerussite completely dissolved under the simulated stomach conditions (Fig. 4.2). The high solubility of hydrocerussite is probably the reason no significant difference was observed between spiking methods for bioaccessible Pb levels. The results showed that it was almost as soluble as PbO and outer-sphere Pb in the oxide and nitrate spiked soils, respectively (Fig.4.2). In addition, this finding further supports the suggestion that the fraction of very soluble metal species in soils affects the bioaccessible metal concentration. This is can be clearly observed by comparing the bioaccessible Pb concentrations between mixtures; the Sudbury mixture, which contained the highest Pb loading, yielded significantly higher bioaccessible Pb concentrations than the Flin Flon and Port Colborne mixtures (Fig. 4.2).

The XANES and LCF analysis showed that secondary Zn species were detected in the simulated stomach and duodenum. In the stomach, $ZnCl_2$ was found in all the residual pellets, indicating that a fraction of the Zn^{2+} ions released during the digestion reacted with Cl^- ions. In the duodenum, both $ZnCl_2$ and $ZnCO_3$ were detected in all the residual pellets (Tables 4.2, 4.3, 4.4, and 4.5). The formation of these precipitates is partly responsible for the low bioaccessible concentrations observed in the duodenum. Also, these results suggest that in the actual stomach and duodenum, aqueous metal ions may form complexes with ligands and other gastrointestinal substances; consequently, this may affect the absorption of the metal ions via the intestinal epithelium. It was observed in the WTRS spiked soils that a fraction of Zn was adsorbed on goethite [FeO(OH)] (Table 4.4). The fraction of Zn adsorbed on goethite was increased in the duodenal residual pellets from the annealed and oxide spiked soils (Table 4.4). It is possible that the deprotonation of the goethite surface as pH increased from 1.4 to 6.3, and the decrease in H^+ ion concentration in the duodenal fluid led to more Zn^{2+} adsorption onto the goethite surface. This may have contributed to the reduction in the bioaccessible Zn concentration in the duodenum (Table 4.4). This observation suggests that for metal contaminated soils containing oxy-hydroxides of Fe, Al, or Mn, adsorption of metal ions is likely to occur as the stomach digestive juice and its contents are gradually transported into the small intestine.

4.6.2 Implications for risk assessment and soil remediation

With regards to soil ingestion, children are the most vulnerable due to their frequent hand-to mouth behavior; they are also the most susceptible to metal toxicity, especially Pb. Hence, it is imperative to determine how much of a potentially toxic metal a child can be exposed to before adverse health effects manifest. The dose rate (internal dose rate for metals) is computed from a number of parameters including the fraction of a metal absorbed into systemic circulation. Risk assessment often assume the bioavailable fraction based on the total metal concentration; in some cases, this value is derived from toxicity studies that use the soluble forms of a metal contaminant, and the dosing vehicle is either food or water. The assumed value is sometimes adjusted to that derived from the toxicity study to account for the difference in dosing medium. These approaches may lead to a high bioavailable fraction, and eventually an overestimation of risk. The current study, by help of synchrotron techniques, has shown that in

most cases, different species of a metal are present in a contaminated soil. The simple bioaccessibility tests conducted demonstrated that the different species do not equally contribute to bioaccessibility: ZnO, sphalerite and outer-sphere Zn contributed more to Zn bioaccessibility than franklinite and Zn-HIM. Hydrocerussite and PbO were also found to contribute towards Pb bioaccessibility. In addition, bioaccessible metal concentrations can be reduced as a result of the formation of precipitates between metal ions and ligands in the GIT. These results lend support to previous research (Ruby et al., 1999; Reeder, Schoonen, & Lanzirotti, 2006; Scheckel et al., 2009; Walraven et al., 2015) that suggested that metal bioaccessibility is controlled by the speciation of metals in soils. Besides, the current study has demonstrated that synchrotron techniques can be useful in risk assessment and contaminated soil remediation. For instance, soils contaminated with predominantly franklinite and/or Zn-HIM will cost less to clean up; however, long-term monitoring of soil conditions is required to ensure the stability of these Zn species. On the other hand, soils with high soluble metal fractions require immediate remediation in order to limit exposure. The formation of stable Zn species after the implementation of a remediation technique can serve as an indication of the effectiveness of the technique. Hamilton et al (2016) reported that recolonization of Zn contaminated soils by native plant species after the application of dolostone was probably due to the formation of Zn-HIM coprecipitates. Precipitation of Zn-HIM lead to a reduction in $CaCl_2$-extractable Zn, and possibly, a reduction in the amount of Zn ions taken up by plants and soil microbes (Hamilton et al., 2016b).

4.7 Conclusions

It has been demonstrated that total metal concentration does not control the amount of a potentially toxic metal that is released from the soil matrix into simulated fluids. Instead, the species of a metal and their relative abundance, soil properties, and conditions in the GIT are the factors that determine a metal's bioaccessible concentration. Concerning a metal species and its relative abundance, a high concentration of a soluble metal species is likely to translate into a high bioaccessible metal concentration. On the other hand, the relative abundance of an insoluble metal species will have little effect on the amount of metal ions released into the digestive juice. Soils with very reactive clay and oxy-hydroxide minerals are likely to adsorb metal ions as the chyme (digestive juice and its contents) makes its passage from the pH 1.4 stomach to the

pH 6.4 duodenum. This coupled with the precipitation of metal ions with ligands and the possible formation of organo-metal complexes in the duodenum will reduce the bioaccessible metal concentration. It thus follow that basing risk assessment on total metal concentration is not an appropriate approach.

5 SYNTHESIS AND CONCLUSIONS

Soil toxicity and risk assessment studies should, ideally, use soil samples from contaminated sites. In cases where field contaminated soils cannot be obtained, the soil spiking method employed must mimic field conditions regarding metal speciation and concentration. In Chapter 3, three soil spiking methods (metal-salt, metal oxide and annealed metal) were evaluated to determine the one that adequately mimic field contaminated soils regarding metal speciation and concentration. The former is very important because it controls the bioavailability and toxicity of metals (Basgta et al., 2005). It was hypothesized that the annealed spiking method better mimics field contaminated conditions.

The commonly used method of adding metal salts to uncontaminated soils and leaching with artificial rainwater to rid the soil of the salts, aside from not mimicking field conditions, also creates artifacts that may skew toxicity results. At low soil pH, H^+ ions occupy most of the adsorption sites hence a significant fraction of the aqueous metal ions added will remain in the soil solution. As the soil is inundated with artificial rainwater, the free metal ions and other basic cations will be inadvertently leached out of the soil. In addition, colloids may be leached out of the soil matrix. However, metals (e.g., Pb) that form relatively stable bonds with organic substances (provided they are present in the test soils) may persist. In clay soils, the over-saturation of the soils is likely to create an anaerobic environment, which will adversely impact the population of obligate aerobes. This alteration of soil physical, chemical and biological properties by the metal salt spiking method may have far-reaching effects on the results of soil toxicity studies. On a practical note, this method may prove to be time consuming for clay soils; the small pore sizes in clay soils, require a very long period to reduce the EC of the metal-salt spiked soils to their control values. Because of the problems generated by leaching, some researches avoid leaching metal-salt spiked soils. This may seem to be a better approach, but aside from altering the soil pH and EC, it may also produce metal bioavailable concentrations that are not representative of field conditions. In contrary to the metal-salt method, the alternative spiking methods (oxide

and annealed) alter soil properties to a lesser degree. For the oxide spiking method, the dissolution of the oxide particles increases the pH of the soil surrounding the oxide particles; this increase in pH is negligible, except when there is a very high relative abundance of metal oxides. The release of metal ions from metal bearing primary minerals reduces soil pH, but the rate of metal release is very slow and hence a drastic reduction in soil pH is not likely to occur. One limitation of the oxide and annealed spiking method is the number of metal species produced. Metal oxides and metal bearing primary minerals are insoluble at neutral and alkaline pH; this implies that in test soils with pH ≥ 7, the metal oxide and primary mineral will be the only species present in the oxide and annealed spiked soils, respectively. These two metal species are not representative of all metal forms in filed contaminated soils. At low pH, the relatively high solubility of metal oxides may result in bioavailable concentrations that are higher than those found in field contaminated soils. On the other hand, the relatively low solubility of metal bearing primary minerals, even at low pH, may result in bioavailable metal concentrations lower than those observed in field contaminated soils.

From the above discussion, it can be inferred that no individual spiking method adequately mimics field contaminated soils. For this reason, a combination of spiking methods is suggested. For instance, Morin et al (1999) used EXAFS to characterize the speciation of Pb in a mine tailing; the 8530 mg Pb kg^{-1} contained in the tailing consisted of 53% Pb sorbed on goethite, 27% pyromorphite [$Pb_5(PO_4)_3Cl$] and 8% hydrocerussite [$Pb_3(CO_3)_2(OH)_2$]. The pH of the tailing was near neutral (pH 6-8) due to the abundance of carbonate (Morin et al., 1999). To adequately mimic such conditions with the aim of determining the potential risks posed by the tailing, a test soil with pH between 6-8 and high carbonate content is required. Pb sorbed on goethite can be synthesized, and its relative concentration added to the test soil. Pyromorphite and hydrocerussite can either be synthesized or purchased and added to the test soil. Afterwards, XAS analysis can be conducted to ascertain the presence of these Pb species in the spiked soil. This approach may prove expensive and laborious, but it is probably the only means by which field contaminated soils can be adequately mimicked. It is suggested that further studies should be carried out to test the feasibility and reproducibility of this approach.

Two kinetic processes control the amount of a potentially toxic metal that is distributed to target organs; in the case of metal ingestion, the first process is the dissolution and release of metal ions into the digestive fluid, followed by the absorption of the metal ions into systemic circulation. Either the former or the latter can be rate limiting (Scheckel et al., 2009). The release of metal ions into digestive fluids has been reported to depend on metal speciation. However, metal speciation studies only make broad predictions concerning the relationship between metal speciation and bioaccessible concentration (Scheckel et al., 2009). And due to the lack of data regarding the metal species that contribute to bioaccessibility, risk assessors often assume values for the fraction of metal ions released from the soil matrix into digestive juices based on the total metal content.

In Chapter 4, it was demonstrated that bioaccssibility tests in conjunction with synchrotron-based speciation studies can provide a reliable basis for the estimation of metal exposure to humans. After characterizing the speciation of Zn in the spiked soils in chapter 3, bioaccessibility tests and XANES analysis were carried out to identify the species of Zn that contribute to bioaccessible concentrations. Prior to this study, it was expected that soluble Zn species will contribute more Zn ions into the simulated digestive juices. The results confirmed this hypothesis: soluble species including ZnO, sphalerite and outer-sphere Zn were found to release more Zn ions into digestive juices than sparingly soluble species such as franklinite and Zn-HIM. Also, it was inferred that soluble Pb species including PbO and hydrocerussite readily released Pb ions into the *in vitro* digestive fluids. Furthermore, the level of Zn and Pb released into the duodenal juice was found to be reduced as a result of precipitation and adsorption reactions. These results have profound implications for risk assessment and the selection and implementation of soil remediation techniques. For instance, for soils contaminated with predominantly sparingly soluble metal species (e.g., franklinite), deriving the bioaccessible fraction from the total metal content will result in an overestimation of risk. Consequently, the cost of remediation will be overestimated, and resources that should be used to clean up high risk sites would be wasted on low risk soils. Exposure to insoluble metal species in soils can be kept at a minimum through monitoring and adjusting (when necessary) soil conditions, especially soil pH, to maintain the stability of the insoluble metal species. In contrast, basing metal bioaccessibility on total metal content

may result in the underestimation of risk in soils containing high concentrations of soluble metal species. This will lead to the underestimation of remediation cost, which may lead to the selection and implementation of the wrong remediation technique.

This current study identified just a few Zn and Pb species that contribute to bioaccessibility under fasting stomach and duodenal conditions, and these metal species may not be present in every field contaminated soil. Also, the *in vitro* digestion models used in this study were relatively simple, and did not consider many gastrointestinal variables that may impact metal release from the soil matrix. These limitations, however, do not take away from the fact that complementing bioaccessibillity tests with synchrotron-based speciation studies is a more robust approach to quantifying the risks associated with metal contaminated soils. It is suggested that in future studies, complex *in vitro* (e.g. SHIME) or *in vivo* models should be tested as well.

6 REFERENCES

Acero, P., Cama, J., & Ayora, C. (2007). Sphalerite dissolution kinetics in acidic environment. *Applied Geochemistry*, *22*(9), 1872–1883.

Adamo, P. & Zampella, M. (2008). Chemical speciation to assess potentially toxic metals'(PTMs') bioavailability and geochemical forms in polluted soils. *Environmental geochemistry, Site Characterization, Data Analysis and Case Histories*, 175–212.

Apostoli, P., Cornelis, J. D., Hoet, P., Lison, D., & Templeton, D. (2006). Elemental speciation in human health risk assessment. *Geneva: World Health Organization*.

Backes, C. A., McLaren, R. G., Rate, A. W., & Swift, R. S. (1995). Kinetics of cadmium and cobalt desorption from iron and manganese oxides. *Soil Science Society of America Journal*, *59*(3), 778–785.

Barceloux, D. G. & Barceloux, D. (1999a). Nickel. *Journal of Toxicology: Clinical Toxicology*, *37*(2), 239–258.

Barceloux, D. G. & Barceloux, D. (1999b). Zinc. *Journal of Toxicology, Clinical Toxicology*, *37*(2), 279–292.

Basta, N., Ryan, J., & Chaney, R. (2005). Trace element chemistry in residual-treated soil. *Journal of Environmental Quality*, *34*(1), 49–63.

Bates, D., MÃd'chler, M., Bolker, B., & Walker, S. (2015). Fitting linear mixed-effects models using lme4. *Journal of Statistical Software*, *67*(1), 1–48. doi:10.18637/jss.v067.i01

Belanger, N., Pare, D., & Hendershot, W. H. (2012). Determining nutrient availability in forest soils. in m.r. carter & e.g. gregorich: Soil sampling and methods of analysis. (Second, pp. 323–324). CRC Press.

Bragg, L. (1968). X-ray crystallography. *Scientific American*, *219*(1), 58–74.

Broos, K., Warne, M. S. J., Heemsbergen, D. A., Stevens, D., Barnes, M. B., Correll, R. L., & McLaughlin, M. J. (2007). Soil factors controlling the toxicity of copper and zinc to microbial processes in australian soils. *Environmental Toxicology and Chemistry*, *26*(4), 583–590.

Brown Jr, G. E. & Parks, G. A. (2001). Sorption of trace elements on mineral surfaces: Modern perspectives from spectroscopic studies, and comments on sorption in the marine environment. *International Geology Review*, *43*(11), 963–1073.

Brown, G. & Brindley, G. W. (1980). *Crystal structures of clay minerals and their x-ray identification*. Mineralogical Society London.

Cao, X., Ma, L. Q., Singh, S. P., & Zhou, Q. (2008). Phosphate-induced lead immobilization from different lead minerals in soils under varying pH conditions. *Environmental Pollution*, *152*(1), 184–192. doi:https://doi.org/10.1016/j.envpol.2007.05.008

Chuan, M., Shu, G., & Liu, J. (1996). Solubility of heavy metals in a contaminated soil: Effects of redox potential and ph. *Water, Air, & Soil Pollution*, *90*(3), 543–556.

Dan, T., Hale, B., Johnson, D., Conard, B., Stiebel, B., & Veska, E. (2008). Toxicity thresholds for oat (Avena sativa L.) grown in Ni-impacted agricultural soils near Port Colborne, Ontario, Canada. *Canadian Journal of Soil Science*, *88*(3), 389–398.

Elzinga, E., Peak, D., & Sparks, D. (2001). Spectroscopic studies of Pb(II)-sulfate interactions at the goethite-water interface. *Geochimica et Cosmochimica Acta*, *65*(14), 2219–2230.

Environment Canada. (2007). Soil pH measurement. *Ottawa: Environment Canada*.

Ford, R. G., Scheinost, A. C., Scheckel, K. G., & Sparks, D. L. (1999). The link between clay mineral weathering and the stabilization of ni surface precipitates. *Environmental Science & Technology*, *33*(18), 3140–3144.

Ford, R. G. & Sparks, D. L. [Donald L]. (2000). The nature of zn precipitates formed in the presence of pyrophyllite. *Environmental science & Technology*, *34*(12), 2479–2483.

Ford, R. G., Sparks, D. L. [Donald L] et al. (2001). Frontiers in metal sorption/precipitation mechanisms on soil mineral surfaces. *Advances in Agronomy*, *74*, 41–62.

Hamilton, J. G., Farrell, R. E., Chen, N., Feng, R., Reid, J., & Peak, D. (2016a). Characterizing zinc speciation in soils from a smelter-affected boreal forest ecosystem. *Journal of Environmental Quality*, *45*(2), 684–692.

Hamilton, J. G., Farrell, R. E., Chen, N., Reid, J., Feng, R., & Peak, D. (2016b). Effects of dolomitic limestone application on zinc speciation in boreal forest smelter-contaminated soils. *Journal of Environmental Quality*, *45*(6), 1894–1900.

Health Canada. (2004). Federal contaminated site risk assessment in canada. part ii: Health canada toxicological reference values. *Ministry of Heath, Ottawa, Canada*.

Health Canada. (2010). Federal contaminated site risk assessment in canada, part v: Guidance on human health detailed quantitative risk assessment for chemicals (dqrachem.) *Ministry of Health, Ottawa, Canada*.

Hogg, D. S., McLaren, R. G., & Swift, R. S. (1993). Desorption of copper from some new zealand soils. *Soil Science Society of America Journal*, *57*(2), 361–366.

ICMM. (2012). Trends in the mining and metals industry. *Mining's contribution to sustainable development*, London, UK: International Counsil on Mining and Metals.

Jacquat, O., Voegelin, A., Juillot, F., & Kretzschmar, R. (2009a). Changes in zn speciation during soil formation from zn-rich limestones. *Geochimica et Cosmochimica Acta*, *73*(19), 5554–5571.

Jacquat, O., Voegelin, A., & Kretzschmar, R. (2009b). Local coordination of zn in hydroxy-interlayered minerals and implications for zn retention in soils. *Geochimica et Cosmochimica Acta*, *73*(2), 348–363.

Jacquat, O., Voegelin, A., & Kretzschmar, R. (2009c). Soil properties controlling zn speciation and fractionation in contaminated soils. *Geochimica et Cosmochimica Acta*, *73*(18), 5256–5272.

JÃÿrgensen, S. S. & Willems, M. (1987). The fate of lead in soils: The transformation of lead pellets in shooting-range soils. *Ambio*, 11–15.

Kelley, N. E., Brauning, S. E., Schoof, R. A., & Ruby, M. V. (2002). *Assessing oral Bioavailability of metals in soil*. Columbus, OH, USA: Battelle Press.

Koch, I., Reimer, K. J., Bakker, M. I., Basta, N. T. [Nicholas T], Cave, M. R., Denys, S., ... Lowney, Y. W., et al. (2013). Variability of bioaccessibility results using seventeen different methods on a standard reference material, NIST 2710. *Journal of Environmental Science and Health, Part A*, *48*(6), 641–655.

Laird, B. D., Weiseth, B., Packull-McCormick, S. R., Peak, D., Dodd, M., & Siciliano, S. D. (2015). Solid-liquid separation method governs the in vitro bioaccessibility of metals in contaminated soil-like test materials. *Chemosphere*, *134*, 544–549.

Li, B., Ma, Y., Mclaughlin, M. J., Kirby, J. K., Cozens, G., & Liu, J. (2010). Influences of soil properties and leaching on copper toxicity to barley root elongation. *Environmental Toxicology and Chemistry*, *29*(4), 835–842.

Lu, P., Nuhfer, N. T., Kelly, S., Li, Q., Konishi, H., Elswick, E., & Zhu, C. (2011). Lead coprecipitation with iron oxyhydroxide nano-particles. *Geochimica et Cosmochimica Acta*, *75*(16), 4547–4561.

Manceau, A., Boisset, M.-C., Sarret, G., Hazemann, J.-L., Mench, M., Cambier, P., & Prost, R. (1996). Direct determination of lead speciation in contaminated soils by exafs spectroscopy. *Environmental Science & Technology*, *30*(5), 1540–1552.

Manceau, A., Lanson, B., Schlegel, M. L., Harge, J. C., Musso, M., Eybert-Berard, L., ... Lamble, G. M. (2000). Quantitative zn speciation in smelter-contaminated soils by exafs spectroscopy. *American Journal of Science*, *300*(4), 289–343.

Manceau, A., Marcus, M. A., & Tamura, N. (2002). Quantitative speciation of heavy metals in soils and sediments by synchrotron x-ray techniques. *Reviews in Mineralogy and Geochemistry*, *49*(1), 341–428.

Manceau, A., Marcus, M. A., Tamura, N., Proux, O., Geoffroy, N., & Lanson, B. (2004). Natural speciation of Zn at the micrometer scale in a clayey soil using X-ray fluorescence, absorption, and diffraction. *Geochimica et Cosmochimica Acta*, *68*(11), 2467–2483.

Matocha, C. J., Elzinga, E. J., & Sparks, D. L. (2001). Reactivity of pb (ii) at the mn (iii, iv)(oxyhydr) oxide- water interface. *Environmental Science & Technology*, *35*(14), 2967–2972.

McMartin, I., Henderson, P., & Nielsen, E. (1999). Impact of a base metal smelter on the geochemistry of soils of the flin flon region, manitoba and saskatchewan. *Canadian Journal of Earth Sciences*, *36*(2), 141–160.

Mertens, J., Broos, K., Wakelin, S. A., Kowalchuk, G. A., Springael, D., & Smolders, E. (2009). Bacteria, not archaea, restore nitrification in a zinc-contaminated soil. *The ISME Journal*, *3*(8), 916–923.

Morin, G., Ostergren, J. D., Juillot, F., Ildefonse, P., Calas, G., & Brown, G. E. (1999). Xafs determination of the chemical form of lead in smelter-contaminated soils and mine tailings: Importance of adsorption processes. *American Mineralogist*, *84*(3), 420–434.

Nachtegaal, M., Marcus, M., Sonke, J., Vangronsveld, J., Livi, K., van Der Lelie, D., & Sparks, D. (2005). Effects of in situ remediation on the speciation and bioavailability of zinc in a smelter contaminated soil. *Geochimica et Cosmochimica Acta*, *69*(19), 4649–4664.

Nriagu, J. (2011). Zinc Toxicity in Humans. *Encyclopedia of Environmental Health*, 801–807. doi:10.1016/B978-0-444-52272-6.00675-9

Nunez, C. & ViÃśals, J. (1984). Kinetics of leaching of zinc ferrite in aqueous hydrochloric acid solutions. *Metallurgical Transactions B*, *15*(2), 221–228.

O'Day, P. A. (1999). Molecular environmental geochemistry. *Reviews of Geophysics*, *37*(2), 249–274.

Oomen, A. G., Hack, A., Minekus, M., Zeijdner, E., Cornelis, C., Schoeters, G., ... Rompelberg, C. J., et al. (2002). Comparison of five in vitro digestion models to study the bioaccessibility of soil contaminants. *Environmental Science & Technology*, *36*(15), 3326–3334.

Ostergren, J. D., Brown, G. E., Parks, G. A., & Tingle, T. N. (1999). Quantitative speciation of lead in selected mine tailings from leadville, co. *Environmental Science & Technology*, *33*(10), 1627–1636.

R Core Team. (2017). *R: A language and environment for statistical computing*. R Foundation for Statistical Computing. Vienna, Austria. Retrieved from https://www.R-project.org

Ravel, B. & Newville, M. (2005). ATHENA, ARTEMIS, HEPHAESTUS: Data analysis for x-ray absorption spectroscopy using ifeffit. *Journal of Synchrotron Radiation*, *12*(4), 537–541.

Reeder, R. J., Schoonen, M. A., & Lanzirotti, A. (2006). Metal speciation and its role in bioaccessibility and bioavailability. *Reviews in Mineralogy and Geochemistry*, *64*(1), 59–113.

Rehr, J. J. & Albers, R. C. (2000). Theoretical approaches to X-ray absorption fine structure. *Reviews of Modern Physics*, *72*(3), 621.

Richardson, G. M., Bright, D. A., & Dodd, M. (2006). Do current standards of practice in canada measure what is relevant to human exposure at contaminated sites? II: oral bioaccessibility of contaminants in soil. *Human and Ecological Risk Assessment*, *12*(3), 606–616.

Ruby, M. V., Schoof, R., Brattin, W., Goldade, M., Post, G., Harnois, M., ... Carpenter, M., et al. (1999). Advances in evaluating the oral bioavailability of inorganics in soil for use in human health risk assessment. *Environmental Science & Technology*, *33*(21), 3697–3705.

Ruyters, S., Mertens, J., Springael, D., & Smolders, E. (2010). Stimulated activity of the soil nitrifying community accelerates community adaptation to zn stress. *Soil Biology and Biochemistry*, *42*(5), 766–772.

Scheckel, K. G., Chaney, R. L., Basta, N. T., & Ryan, J. A. (2009). Advances in assessing bioavailability of metal(loid)s in contaminated soils. *Advances in Agronomy*, *104*, 1–52.

Scheckel, K. G., Scheinost, A. C., Ford, R. G., & Sparks, D. L. (2000). Stability of layered Ni hydroxide surface precipitates-A dissolution kinetics study. *Geochimica et Cosmochimica Acta*, *64*(16), 2727–2735.

Scheckel, K. G. & Sparks, D. L. [Donald L]. (2001). Dissolution kinetics of nickel surface precipitates on clay mineral and oxide surfaces. *Soil Science Society of America Journal*, *65*(3), 685–694.

Scheidegger, A. & Sparks, D. (1996). Kinetics of the formation and the dissolution of nickel surface precipitates on pyrophyllite. *Chemical Geology*, *132*(1-4), 157–164.

Scheinost, A. C., Kretzschmar, R., Pfister, S., & Roberts, D. R. (2002). Combining selective sequential extractions, x-ray absorption spectroscopy, and principal component analysis for quantitative zinc speciation in soil. *Environmental Science & Technology*, *36*(23), 5021–5028.

Seshadri, B., Bolan, N., & Naidu, R. (2015). Rhizosphere-induced heavy metal (loid) transformation in relation to bioavailability and remediation. *Journal of Soil Science and Plant Nutrition*, *15*(2), 524–548.

Sivry, Y., Munoz, M., Sappin-Didier, V., Riotte, J., Denaix, L., De Parseval, P., ... DuprÃĽ, B. (2010). Multimetallic contamination from Zn-ore smelter: Solid speciation and potential mobility in riverine floodbank soils of the upper lot river (SW France). *European Journal of Mineralogy*, *22*(5), 679–691.

Smith, K. S. (1999). Metal sorption on mineral surfaces: An overview with examples relating to mineral deposits. *The environmental geochemistry of mineral deposits. Reviews in Economic Geology*, *6*, 161–182.

Sparks, D. [D.]. (2003). *Environmental Soil Chemistry: Second Edition*. Academic press.

Stanton, M. R., Gemery-Hill, P. A., Shanks III, W. C., & Taylor, C. D. (2008). Rates of zinc and trace metal release from dissolving sphalerite at ph 2.0–4.0. *Applied Geochemistry*, *23*(2), 136–147.

Sudbury Smelter Business Unit and Falconbridge, ON. (2004). Metal levels in the soils of the sudbury smelter footprint. *Sudbury Regional Soils Project. Centre for Environmental Monitoring*. Retrieved from http://www.sudburysoilsstudy.com/en/media/support/reports/2001soilsdata/vol_ii/cem_report1-61.pdf

Templeton, D. M., Ariese, F., Cornelis, R., Danielsson, L.-G., Muntau, H., van Leeuwen, H. P., & Lobinski, R. (2000). Guidelines for terms related to chemical speciation and fractionation of elements. definitions, structural aspects, and methodological approaches (iupac recommendations 2000). *Pure and Applied Chemistry*, *72*(8), 1453–1470.

Toby, B. H. & Von Dreele, R. B. (2013). GSAS-II: The genesis of a modern open-source all purpose crystallography software package. *Journal of Applied Crystallography*, *46*(2), 544–549.

Traina, S. J. & Laperche, V. (1999). Contaminant bioavailability in soils, sediments, and aquatic environments. *Proceedings of the National Academy of Sciences*, *96*(7), 3365–3371.

USEPA. (2007). Guidance for evaluating the oral bioavailability of met-als in soils for use in human health risk assessment. *Washington DC*.

Voegelin, A., Jacquat, O., Pfister, S., Barmettler, K., Scheinost, A. C., & Kretzschmar, R. (2011). Time-dependent changes of zinc speciation in four soils contaminated with zincite or sphalerite. *Environmental Science & Technology*, *45*(1), 255–261.

Voegelin, A., Pfister, S., Scheinost, A. C., Marcus, M. A., & Kretzschmar, R. (2005). Changes in zinc speciation in field soil after contamination with zinc oxide. *Environmental Science & Technology*, *39*(17), 6616–6623.

Voegelin, A., Scheinost, A. C., BÃijhlmann, K., Barmettler, K., & Kretzschmar, R. (2002). Slow formation and dissolution of Zn precipitates in soil: A combined column-

transport and xafs study. *Environmental Science & Technology*, *36*(17), 3749–3754.

Walraven, N., Bakker, M., van Os, B., Klaver, G., Middelburg, J., & Davies, G. (2015). Factors controlling the oral bioaccessibility of anthropogenic Pb in polluted soils. *Science of The Total Environment*, *506-507*, 149–163. doi:https://doi.org/10.1016/j.scitotenv.2014.10.118

Weisener, C., Smart, R., & Gerson, A. (2003). Kinetics and mechanisms of the leaching of low Fe sphalerite. *Geochimica et Cosmochimica Acta*, *67*(5), 823–830. Advances in Oxide and Sulfide Mineral Surface Chemistry. doi:https://doi.org/10.1016/S0016-7037(02)01276-0

WHO. (1996). Biological monitoring of chemical exposure in the workplace: Guidelines. *Geneva: World Health Organization*.

Williams, C., Walton, G., Jiang, L., Plummer, S., Garaiova, I., & Gibson, G. R. (2015). Comparative analysis of intestinal tract models. *Annual Review of Food Science and Technology*, *6*, 329–350.

Xia, K., Bleam, W., & Helmke, P. A. (1997). Studies of the nature of Cu^{2+} and Pb^{2+} binding sites in soil humic substances using x-ray absorption spectroscopy. *Geochimica et Cosmochimica Acta*, *61*(11), 2211–2221.

Yano, J. & Yachandra, V. K. (2009). X-ray absorption spectroscopy. *Photosynthesis Research*, *102*(2-3), 241.

Zhang, G. & Peak, D. (2007). Studies of Cd(II)-sulfate interactions at the goethite-water interface by atr-ftir spectroscopy. *Geochimica et Cosmochimica Acta*, *71*(9), 2158–2169.

Zia, M. H., Codling, E. E., Scheckel, K. G., & Chaney, R. L. (2011). In vitro and in vivo approaches for the measurement of oral bioavailability of lead (pb) in contaminated soils: A review. *Environmental Pollution*, *159*(10), 2320–2327. Nitrogen Deposition, Critical Loads and Biodiversity. doi:https://doi.org/10.1016/j.envpol.2011.04.043

A Appendix

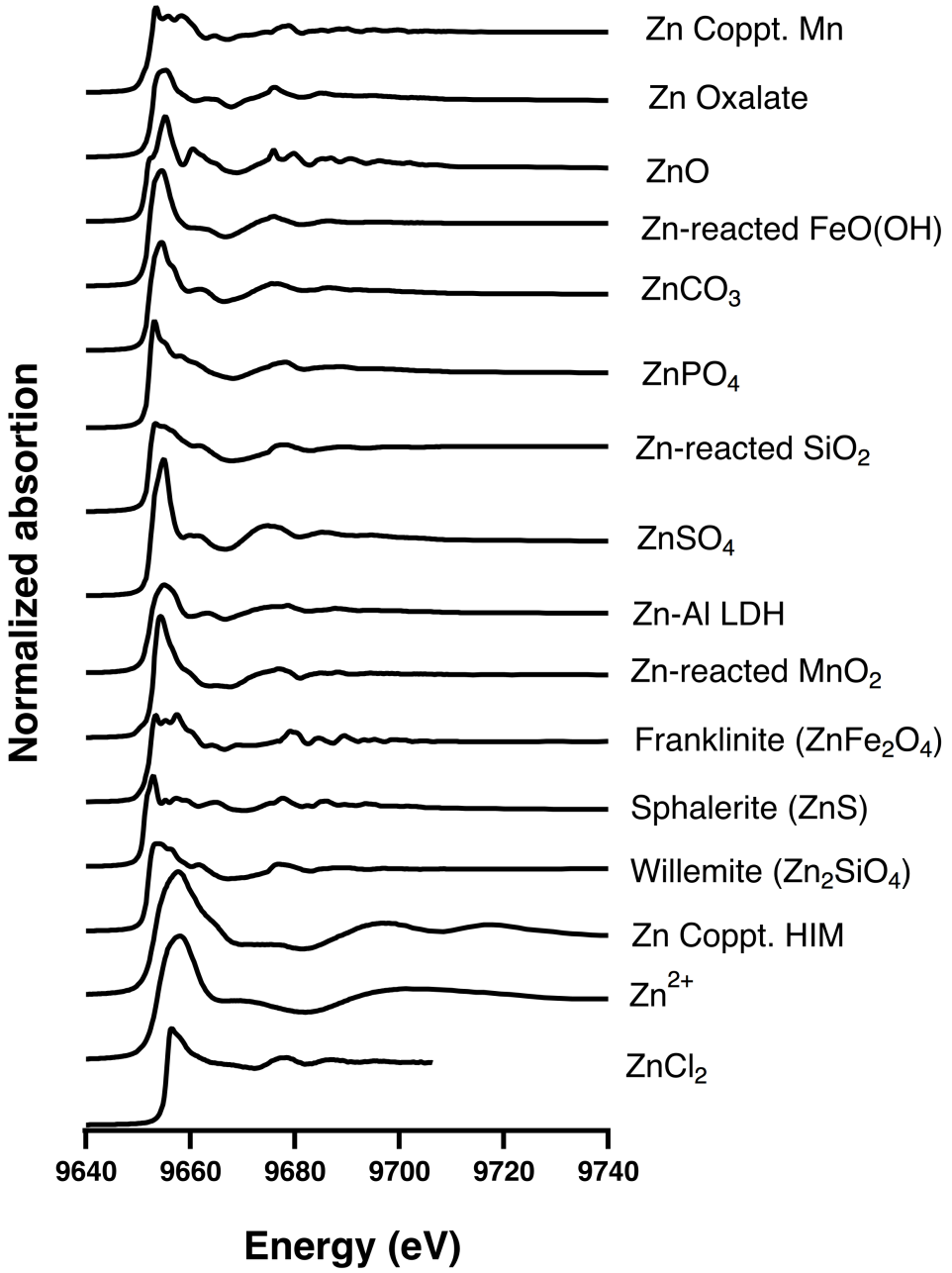

Fig. A.1: Zn reference standards bulk XANES used in linear combination fitting of spiked and smelter-affected soils, and residual pellets.

Table A.1: ANOVA table: gastric Zn bioaccessibility

Source of variation	SS	MS	df	F	p
soil	0.22	0.11	2	2442.30	< 0.001
sm[†]	1.25	0.63	2	13691.1 1	< 0.001
mixture	0.99	0.49	2	10807.13	< 0.001
time	0.02	0.01	2	204.46	< 0.001
soil:sm	0.51	0.13	4	2775.38	< 0.001
soil:mixture	0.28	0.07	4	1544.09	< 0.001
sm:mixture	0.11	0.03	4	591.70	< 0.001
soil:time	0.00	0.00	4	7.45	< 0.001
sm:time	0.01	0.00	4	44.14	< 0.001
satio:time	0.01	0.00	4	44.32	< 0.001
soil:sm:mixture	0.20	0.02	8	540.38	< 0.001
soil:sm:time	0.00	0.00	8	5.70	< 0.001
soil:mixture:time	0.00	0.00	8	9.22	< 0.001
sm:mixture:time	0.00	0.00	8	4.41	< 0.001
soil:sm:mixture:time	0.00	0.00	16	5.54	< 0.001

[†] spiking method

Table A.2: ANOVA table: duodenal Zn bioaccessibility

Source of variation	SS	MS	df	F	p
soil	0.50	0.25	2	99.03	< 0.001
sm[†]	22.95	11.48	2	4528.51	< 0.001
mixture	19.31	9.66	2	3810.77	< 0.001
soil:sm	2.51	0.63	4	247.36	< 0.001
soil:mixture	1.41	0.35	4	138.72	< 0.001
spike:mixture	2.52	0.63	4	248.23	< 0.001
soil:sm:mixture	2.82	0.35	8	138.87	< 0.001

[†] spiking method

Table A.3: ANOVA table: gastric Pb bioaccessibility

Source of variation	SS	MS	df	F	p
soil	0.24	0.12	2	359.28	< 0.001
sm[†]	0.05	0.02	2	75.11	< 0.001
time	0.03	0.01	2	38.76	< 0.001
mixture	11.65	5.83	2	17661.79	< 0.001
soil:sm	0.10	0.02	4	73.04	< 0.001
soil:time	0.00	0.00	4	0.62	0.65
sm:time	0.01	0.00	4	8.73	< 0.001
soil:mixture	0.36	0.09	4	275.66	< 0.001
spike:mixture	0.76	0.19	4	74.85	< 0.001
time:mixture	0.01	0.00	4	9.94	< 0.001
soil:sm:time	0.00	0.00	8	1.61	0.13
soil:spike:mixture	0.23	0.03	8	87.35	< 0.001
soil:time:mixture	0.01	0.00	8	2.30	0.03
sm:time:mixture	0.01	0.00	8	2.01	0.05
soil:sm:time:mixture	0.00	0.00	16	0.70	0.79

[†] spiking method

Table A.4: ANOVA table: gastric Pb bioaccessibility

Source of variation	SS	MS	df	F	p
soil	0.13	0.07	2	239.39	< 0.001
sm[†]	0.00	0.00	2	3.27	0.05
time	0.02	0.01	2	38.99	< 0.001
mixture	3.01	1.50	2	5501.72	< 0.001
soil:sm	0.02	0.00	4	17.53	< 0.001
soil:time	0.01	0.00	4	11.93	< 0.001
sm:time	0.00	0.00	4	0.56	0.69
soil:mixture	0.14	0.03	4	127.56	< 0.001
sm:mixture	0.02	0.01	4	21.81	< 0.001
time:mixture	0.01	0.00	4	10.86	< 0.001
soil:sm:time	0.00	0.00	8	0.38	0.93
soil:sm:mixture	0.05	0.01	8	23.53	< 0.001
soil:time:mixture	0.02	0.00	8	10.90	< 0.001
sm:time:mixture	0.00	0.00	8	1.18	0.31
soil:sm:time:mixture	0.00	0.00	16	0.40	0.98

[†] spiking method

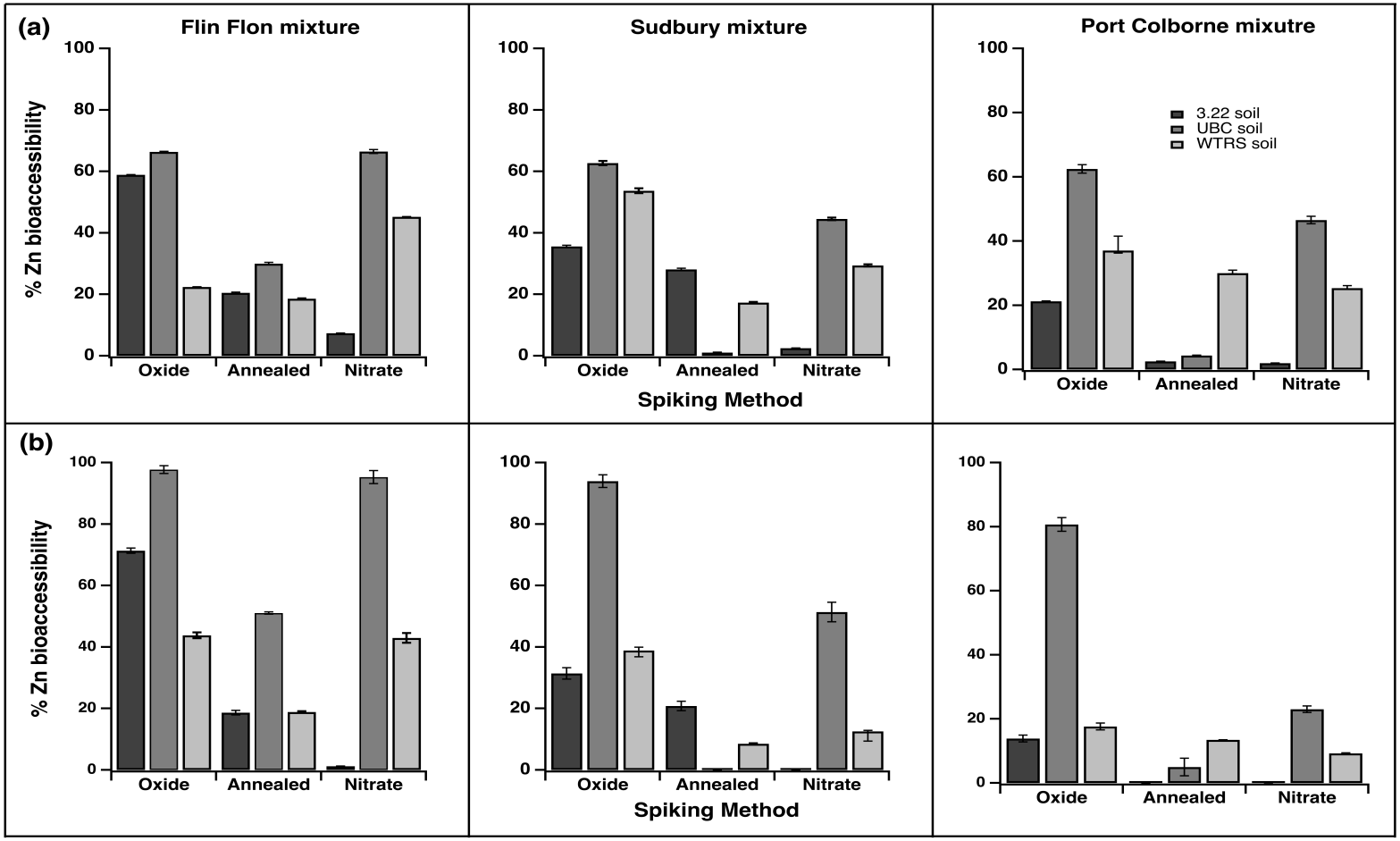

Fig. A.2: Percent Zn compared across 3 factors: mixture (Flin Flon, Sudbury and Port Colborne), spiking method (oxide, annealed, and nitrate) and soil (3.22, UBC, and WTRS). Since time was not a significant predictor of bioaceessibility, only bioaccessible concentrations after 120 and 240 minutes are presented in this graph for stomach and duodenum, respectively. (a) represents stomach and (b) duodenum. Bars with the same lowercase alphabets are not significantly different. Calculation of % Zn bioaccessibility was based on the assumption that 0.1 g of soil was removed at each sampling point.

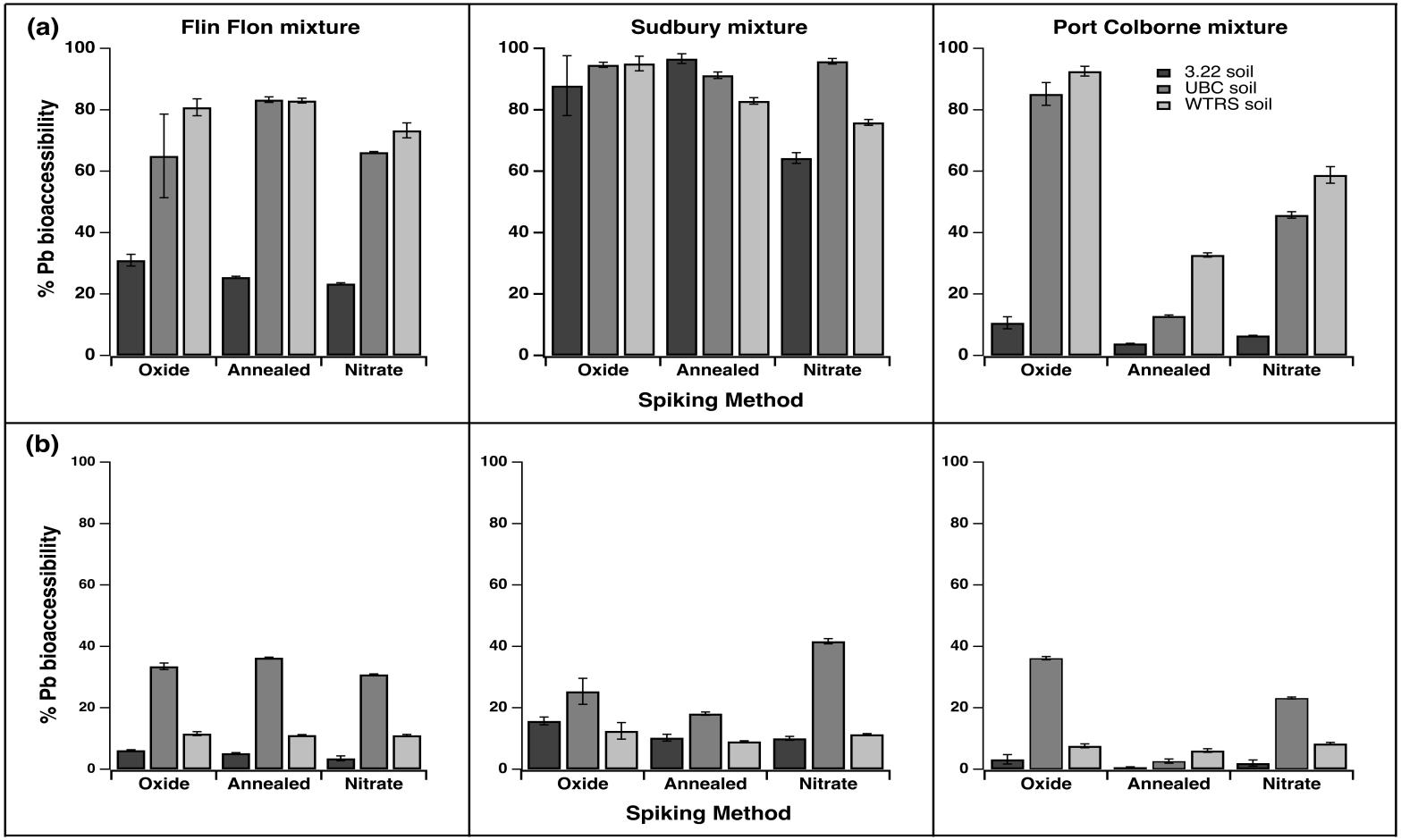

Fig. A.3: Percent Pb bioaccessibility compared across 3 factors: mixture (Flin Flon, Sudbury and Port Colborne), spiking method (oxide, annealed, and nitrate) and soil (3.22, UBC, and WTRS). Since time was not a significant predictor of bioaceessibility, only bioaccessible concentrations after 120 and 240 minutes are presented in this graph for stomach and duodenum, respectively. (a) represents stomach and (b) duodenum. Bars with the same lowercase alphabets are not significantly different. Calculation of % Zn bioaccessibility was based on the assumption that 0.1 g of soil was removed at each sampling point.